

Design and Analysis of Dual Shape Core Large-Mode-Area Leaky Channel Waveguide For High Power Application

A Dissertation submitted towards the partial fulfillment of
the requirement for the award of degree of

Master of Technology

In

Nano Science and Technology

By

Kislay Srivastava

2K11/NST/07

Under the supervision of

Dr. Ajeet Kumar



**DEPARTMENT OF APPLIED PHYSICS
DELHI TECHNOLOGICAL UNIVERSITY**

DELHI – 110042

SESSION 2012-13

CERTIFICATE

This is to certify that the dissertation title “*Design and Analysis of Dual Shape Core Large-Mode-Area Leaky Channel Waveguide For High Power Application*” is the authentic work of **Mr. Kislay Srivastava** under my guidance and supervision in the partial fulfillment of requirement towards the degree of Master of Technology in run by the Department of Applied Physics in *Delhi Technological University*.

Dr. Ajeet Kumar

Supervisor

Assistant Professor

Delhi Technological University

Prof. S.C.Sharma

HOD

Dept. of Applied Physics

Delhi Technological University

DECLARATION BY THE CANDIDATE

I hereby declare that the work presented in this dissertation entitled “**Design and Analysis of Dual Shape Core Large-Mode-Area Leaky Channel Waveguide for High Power Application**” has been carried out by me under the guidance of Dr. Ajeet Kumar, Assistant Professor, Department of Applied Physics, Delhi Technological University, Delhi and hereby submitted for the partial fulfillment for the award of degree of Master of Technology in Nanoscience and Technology at Applied Physics Department, Delhi Technological University, Delhi.

I further undertake that the work embodied in this major project has not been submitted for the award of any other degree elsewhere.

Kislay Srivastava

2K11/NST/07

M.Tech (NST)

ACKNOWLEDGEMENT

I am indebted to my thesis supervisor **Dr. Ajeet Kumar**, Department of Physics, for his gracious encouragement and very valued constructive criticism that has driven me to carry the project successfully.

I am deeply grateful to **Prof. S.C.Sharma**, Head of Department (Applied Physics), Delhi Technological University for his support and encouragement in carrying out this project.

I wish to express my heart full thanks to my branch coordinator **Dr. Pawan Kumar Tyagi** and friends for their goodwill and support that helped me lot in successful completion of this project. This project wouldn't have been completed without the sincere help of research scholar **Mr. Than Singh Saini**.

I express my deep sense of gratitude to my parents **Dr. V. S. Srivastava, Dr. Anita Srivastava** and to my elder brother.

Finally I would like to thank almighty God for his blessings without which nothing is possible in this world.

Kislay Srivastava

M.Tech (NST)

2K11/NST/07

Table of Contents

Certificate	i
Acknowledgement	iii
List of Figures	vi
Abstract	viii
Chapter 1: Introduction	
1.1 Optical Waveguide	1
1.2 Single Mode Propagation	2
1.3 Objectives and Organization of the Thesis	3
Chapter 2: Large-Mode-Area Waveguides and Fibers	
2.1 Introduction	5
2.2 Design Approaches and Limiting Factors for Fibers	6
2.3 A General Difficulty	9
2.4 Recent Developments	9
2.5 Design for LMA operation for Waveguides	11
Chapter 3: Method of Analysis	
3.1 Introduction	16
3.2 Numerical Methods	18

3.3 Finite Element method	18
3.4 Finite Difference Beam Propagation Method	21
3.5 Analytical Methods	22
3.6 Effective Index Method	23
Chapter 4: Design and Analysis of Leaky Channel Waveguide	26
Chapter 5: Conclusion and Scope for Future Work	39
References	41

List of Figures

<i>1.1 Basic structure and refractive-index profile of the optical waveguide</i>	2
<i>2.1 Cross-section of a leaky channel waveguide</i>	11
<i>2.2 Thickness of the cladding varies according to the power-law expression</i>	12
<i>2.3 Stair-case design of a leaky channel waveguide</i>	12
<i>2.4 Design of leaky channel waveguide</i>	13
<i>3.1 Typical dielectric waveguides</i>	15
<i>3.2 Modeling of a buried waveguide using a Finite Element mesh</i>	17
<i>3.3 The Effective Index method for the rib waveguide</i>	22
<i>4.1 Proposed Leaky structure</i>	26
<i>4.2 Contour plot of E_{11}^x</i>	28
<i>4.3 Contour plot of E_{21}^x</i>	28
<i>4.4 Field plot of E_{11}^x</i>	29
<i>4.5 Field plot of E_{11}^y</i>	29
<i>4.6 Field plot of E_{21}^x</i>	30
<i>4.7 Field plot of E_{21}^y</i>	30
<i>4.8 Variation of leakage loss of E_{21}^x and E_{31}^x with d_1</i>	31
<i>4.9 Variation of mode area of E_{21}^x with d_1</i>	32
<i>4.10 Variation of leakage loss of E_{21}^x with d_2</i>	33
<i>4.11 Variation of mode area of E_{21}^x with d_2</i>	34
<i>4.12 Variation of leakage loss of E_{21}^x with t</i>	34
<i>4.13 Variation of mode area of E_{21}^x with t</i>	35
<i>4.14 Variation of leakage loss of E_{21}^x with change in a</i>	36
<i>4.15 Variation of mode area of E_{21}^x with change in a</i>	36
<i>4.16 One-dimensional effective refractive-index profiles</i>	37

4.17 Variation of effective index of $E_{11}^x, E_{21}^x, E_{11}^y$ and E_{21}^y with change in value of wavelength

38

ABSTRACT

We propose a leaky channel waveguide for large-mode-area extended single-mode operation. The proposed structure is characterized by specially designed guiding core and multilayer cladding. Specially designed cladding enables all the supported modes except fundamental modes leaky. Leakage loss of the higher-order mode which is key factor of single-mode operation is calculated by solving the profile by effective index method in conjunction with transfer matrix method. Dispersive cladding of the proposed design makes this design enable to show extended single mode operation in the entire wavelength range beyond 900 nm with a mode area as large as $100\mu\text{m}^2$. Such a large confinement area for mode propagation can effectively suppress non linear optical effects. The waveguide is expected to find application in the design of high power lasers and amplifiers.

Chapter 1

INTRODUCTION

1.1 Optical Waveguide

An optical waveguide [1, 2, 3] is a physical structure that guides electromagnetic waves in the optical spectrum. Common types of optical waveguides include optical fiber and rectangular waveguides. Optical waveguides are used as components in integrated optical circuits or as the transmission medium in local and long haul optical communication systems. Optical waveguides can be classified according to their geometry (planar, strip, or fiber waveguides), mode structure (single-mode, multi-mode), refractive index distribution (step or gradient index) and material (glass, polymer, semiconductor).

Optical fibers and optical waveguides consist of a core, in which light is confined, and a cladding, or substrate surrounding the core, as shown in Fig.1.1. The refractive index of the core n_1 is higher than that of the cladding n_0 . Therefore the light beam that is coupled to the end face of the waveguide is confined in the core by total internal reflection. The condition for total internal reflection at the core-cladding interface is given by $n_1 (\sin \pi/2 - \Phi) \geq n_0$. Since the angle Φ is related with the incident angle θ by $\sin \theta = n_1 \sin \Phi \leq \sqrt{n_1^2 - n_0^2}$, we obtain the critical condition for the total internal reflection as

$$\theta \leq \sin^{-1} \sqrt{n_1^2 - n_0^2} = \theta_{max} \quad (1.1)$$

The refractive-index difference between core and cladding is of the order of $n_1 - n_0 = 0.01$. Then θ_{max} in Eq. (1.1) can be approximated by

$$\theta_{max} = \sqrt{n_1^2 - n_0^2} \quad (1.2)$$

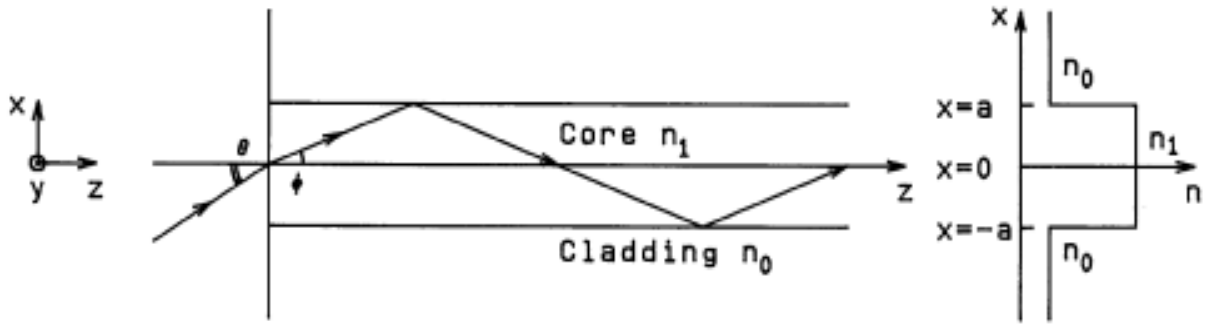


Fig.1.1 Basic structure and refractive-index profile of the optical waveguide

(source: Fundamental of Optical Waveguide: By KATSUNARI OKAMOTO[4])

θ_{max} denotes the maximum light acceptance angle of the waveguide and is known as the numerical aperture (NA).

The relative refractive-index difference between n_1 and n_0 is defined as

$$\Delta = \frac{n_1^2 - n_0^2}{2n_1^2} \cong \frac{n_1 - n_0}{n_0} \quad (1.3)$$

Δ is commonly expressed as a percentage. The numerical aperture NA is related to the relative refractive-index difference Δ by

$$NA = \theta_{max} \cong n_1 \sqrt{2\Delta} \quad (1.4)$$

1.2 Single Mode Propagation

Single mode propagation [4] has the advantage of low intermodal dispersion compared to multimode propagation. The number of guided modes depends upon physical parameters i.e. relative refractive index difference, core radius of the waveguide and wavelength used. The cut off frequency is equal to normalized frequency V for guided modes below which they cannot exist. However mode propagation does not stop below cut off. Modes may propagate as unguided or leaky modes and can travel considerable distances along the waveguide. However guided modes are of paramount importance in optical fiber

communications as these are confined to the fiber over its full length. Total number of guided modes or mode volume for a step index fiber is given by the relation

$$M = \frac{V^2}{2} \quad (1.5)$$

where V is normalized parameter

$$V = \frac{2\pi}{\lambda} a n_1 \sqrt{2\Delta} \quad (1.6)$$

where a is core radius, λ is the wavelength of operation, n_1 is refractive index of core.

For propagation of only single mode, normalized parameter must be in the range of $0 \leq V \leq V_c$, where $V_c = 2.405$.

1.3 Objectives and Organization of the Thesis

This thesis is concerned with the design of a rectangular waveguide for Large-mode-area extended single mode operation. Integrated-optic waveguide lasers have drawn considerable attention for their compactness and possibility of integrating several components. Single mode waveguides are ideal choices for such waveguide lasers in order to prevent mode competition and intermodal dispersion. A conventional single mode waveguide however may give rise to unwanted nonlinear effects due to thin guiding region. There have been attempts to increase the mode areas for applications in high power fiber lasers. We have proposed a leaky cladding structure to provide large-mode-area single-mode operation by introducing large leakage losses to higher-order modes and only a small loss to the fundamental mode.

The thesis consists of five chapters. Each chapter has its own introduction. This dissertation has been ordered in such a way that the process of constructing the rectangular waveguide for large-mode-area extended single mode operation is evident throughout.

Proceeding in a logical manner, **Chapter 2** deals with the ways by which LMA single mode operation can be done, that are known to the world.

Chapter 3 focus is placed on the Method of Analysis, which will include effective index method (EIM) in conjunction with the transfer-matrix-method (TMM).

Chapter 4 deals with the result and simulations for LMA based leaky channel waveguide.

Chapter 5 Finally, the conclusion and scope for the future work are given in this chapter.

Chapter 2

Large-Mode-Area Waveguides and Fibers

2.1 Introduction

Integrated-optic waveguide lasers have drawn considerable attention for their compactness and possibility of device integration [5]. Single-mode waveguides are usually employed in such lasers to avoid mode competition and intermodal dispersion. Single-mode operation also ensures good beam quality, which is essential for engineering applications, especially when the laser is coupled to a single-mode optical fiber. A conventional optical waveguide requires a small core area to provide single-mode operation, where the tight light confinement can reduce the optical damage threshold and, at the same time, give rise to significant unwanted nonlinear optical effects. The preferred waveguide structure for high power applications should have a large single-mode core. In fact, there have been attempts to increase the mode areas in fibers for applications in optical communications and high power fiber lasers and amplifiers. One can increase the effective mode area of a fiber by controlling the refractive index profile in the core or the relative index difference between the core and the cladding [6-7]. Another large-core design is the single material photonic crystal fiber [8], which is characterized by a distribution of air holes in the cladding running through the entire length of fiber. Large-mode-area fibers based on using azimuthally segmented cladding profiles have also been demonstrated [9-11], which do not rely on air holes and can offer mode areas comparable to those of large core holey fibers. In rectangular geometry, large-core single mode waveguides have been achieved by using small index contrast in polymer waveguides [12] and by deep etching in semiconductor waveguides [13]. Recently, we have proposed another principle of achieving large-mode-area single-mode operation in a fiber [14] or a slab waveguide [15] based on creating a leaky graded-index cladding profile. In this chapter, we will be dealing with the ways by which LMA single mode operation can be done, that are known to the world.

2.2 Design Approaches and Limiting Factors for fiber

A straightforward design approach to obtain large mode areas is to decrease the numerical aperture (NA), i.e., to decrease the refractive index difference between the core and the cladding, for a step-index fiber designs. However, there are severe limitations: the guidance (wave guiding) then becomes weak, and significant losses can arise from small imperfections of the fiber or from bending (\rightarrow bend losses). Therefore, the numerical aperture cannot be made smaller than approximately 0.06. To achieve relatively robust single-mode guidance at larger mode areas, there are several more refined design approaches with specially optimized refractive index profiles, which allow for mode areas up to the order of $1000 \mu\text{m}^2$. This is an order of magnitude higher than for ordinary single-mode fibers.

There are additional difficulties in applying this concept to rare-earth-doped fibers. Relatively high concentrations of additional dopants are often required, e.g. for reducing certain quenching effects, and these dopants often increase the numerical aperture. Even if the refractive index contrast can be reduced in some way, the precision of refractive index control may be decreased, and this affects the ability to realize very large mode areas.

Somewhat larger mode areas can be achieved with fiber designs supporting a few propagation modes (\rightarrow multimode fibers). It may then still be possible to guide light dominantly in the fundamental mode, so that the output e.g. of a fiber amplifier is close to diffraction limited [16-18]. Stringent limitations arise from the more critical launch conditions and from mode mixing in the fiber, which can spoil the beam quality and lead to beam pointing fluctuations [19].

Various more sophisticated fiber designs (partly based on photonic crystal fibers) and techniques have been developed for addressing these challenges. In many cases, one attempts to introduce substantial propagation losses for any higher-order modes, making it easier to maintain robust single-mode propagation in a multimode fiber. Another important aspect is to minimize unwanted mode coupling. Some examples for possible strategies are:

- One may strongly bend the fiber; depending on the fiber design, the induced bend losses may be substantial for higher-order modes at a point where they are not yet

significant for the fundamental mode. Fiber designs can be optimized in that respect. Note that bending not only introduces losses, but also can reduce the effective mode area. This is particularly true for large mode area step-index fibers. For a fair comparison of fiber types, this effect definitely has to be taken into account [20]. It turns out that some fiber designs have a large mode area without bending, but a much reduced mode area with bending, whereas there are other designs (e.g. with a parabolic index profile) where the mode area starts with a somewhat smaller value but is much less sensitive to bending.

- So-called chirally coupled core fibers [21,22] have a straight central core in which the signal propagates, plus another core which is helically wound around the central core. It is possible to obtain strongly selective coupling of the helical core only to higher-order modes of the central core, while leaving the fundamental mode essentially unaffected. The principle of this selective coupling is that the helicity affects the propagation constant in such a way that at least in some limited wavelength range phase matching occurs only for coupling to higher-order modes but not to the fundamental mode.
- In leakage channel fibers [23,24], the core is surrounded by a small number of large holes, making all propagation modes leaky in a very selective way, such that all higher-order modes but not the fundamental mode experience substantial propagation losses. While earlier versions of such fibers have been made as photonic crystal fibers with air holes, solid all-glass designs are also possible [25].

The best fiber designs reach an effective mode area of several thousand μm^2 . There is not a strict limit, but designs with larger mode areas exhibit less robust single-mode propagation and often can tolerate only very slight bending. It appears that no kind of design can offer a further substantial expansion of the mode area with robust single-mode propagation. The reason for this is essentially that a mode involves some balance of diffraction and wave guiding, and as diffraction inevitably becomes weaker at larger mode areas, this balance becomes more and more sensitive to any disturbances.

In high-power fiber lasers and amplifiers based on large mode area fibers, thermal lensing can lead to changes of mode properties, in particular to a reduction in effective mode area [26]. The problem of refractive index control can in some situations be mitigated

by using a multifilament core, where the fiber core is realized as a two-dimensional array of filaments [27]. As each single filament exhibits only weak guidance, the overall structure can exhibit single-mode guidance. This concept is particularly interesting for erbium-ytterbium-doped fibers.

An interesting concept described recently [28,29] is first to couple light from the fundamental mode to a particular higher-order mode, using a long-period fiber Bragg grating, then to propagate the light in this higher-order mode in the amplifying fiber, and then finally to convert the light back to the fundamental mode with another fiber Bragg grating. The claimed advantage of using a higher-order mode is twofold: such modes have larger effective mode areas, and they exhibit a weaker coupling to other modes. The power losses associated with coupling to and from this higher-order mode can be small, and the fiber design can be optimized for a broad bandwidth for this coupling. However, difficulties can arise from the very uneven intensity distribution. This can lead to fiber damage even in a regime where the overall nonlinearity is moderately strong, so the approach may solve problems with nonlinearities but not those with damage. Also, the mode field significantly extends into the cladding (the inner cladding in the case of a double-clad fiber), which is not ideal for amplification.

Another novel concept is that of the gain-guided, index-antiguidded single-mode fiber [30-33], which is a type of active fiber. Here, the unpumped fiber is not guiding (even antiguiding), as the refractive index of its core is lower than that of the cladding. For sufficiently strong pumping, however, gain guiding can stabilize a leaky mode with high beam quality. As the losses of such a mode rapidly decrease for increasing core size, a fairly moderate laser gain can be sufficient to achieve propagation with positive net gain if the core is large. Higher-order modes also exist, but would require a significantly higher gain. That level of gain is not reached when the lower-order mode saturates the gain, as it easily happens in a laser, but not necessarily in a high-gain amplifier. The greatest challenge of this concept is efficient pumping. Note that the pump light is not guided and even expelled from the doped core by the index structure and the absorption. A diode-pumped fiber laser has been demonstrated with this concept, but novel pump arrangements will have to be developed to allow for efficient operation.

2.3 A General Difficulty

A general problem with the use of large mode area fibers is that these fibers are not compatible with standard fiber components. (Many fiber-optic components are only available with standard mode sizes.) When a large mode area fiber is fusion spliced to a standard fiber, the large mismatch in mode areas leads to an excessive power loss at the joint. There are two solutions to this problem, which however are both not fully satisfying:

- One can use a tapered fiber as a mode converter between the two fibers. The tapered fiber must be made such that the mode size matches that of the large mode area fiber on one end and that of the standard fiber on the other hand. One then has to do two splices instead of one, but each one can have very low losses. The main difficulty with that method is that a tapered fiber is needed, which may not be easy to obtain.

A frequently used solution for laboratory experiments is to use free-space coupling from and to the large mode area fiber. A laser resonator may then be made with bulk components only, apart from the active fiber. This leads to flexible laboratory setups, which however are not very suitable for commercial use, as they involve sensitive alignment and are sensitive to dust, particularly to dust deposited on the fiber ends.

2.4 RECENT DEVELOPMENTS

High power fiber lasers and amplifiers have of course been a very important topic at various conferences throughout the world. Quite a number of talks addressed the quest for larger mode areas, as this issue has been recognized as the central bottleneck which has to be overcome in order to continue the recent enormous performance enhancements. Quite some creativity has been unleashed in the context of attempts to tackle this problem. These are:

- Sandia National Labs is optimizing refractive index profiles for very large mode areas. Some combined power-law design was found to exhibit better performance than e.g. square-law or triangular profile fibers [33].

- Fitel reported on distributed mode filtering in a cladding-pumped amplifier. This technique makes it possible to suppress higher-order modes as well as to filter out ASE [34].
- Researchers at the University of Michigan, collaborating with the company Nufern, have demonstrated a fiber with chirally-coupled core. This contains a second core wound around the central core. The idea is basically to obtain phase-matched coupling e.g. of the LP₁₁ mode to the lossy chiral core, hoping to suppress all higher-order modes of the multimode core even at large mode areas [35].
- IMRA reported an impressive mode area of about 3000 μm² in an ytterbium-doped leakage channel fiber. This is a photonic crystal fiber made so that the core supports several modes, but higher-order modes are strongly attenuated by leakage through gaps between the air holes [36].
- Femlight uses a 60-cm long rod-type photonic crystal fiber which has to be kept straight. The concept is essentially to live with a very weakly guiding core by avoiding any bending. Quite short pulses with up to 50 W average powers are generated with high efficiency. However, such a device is actually no more used like a normal fiber; it is more like a long bulk crystal with some built-in weak guiding mechanism.
- The probably most radical approach is based on a concept developed by the famous Anthony E. Siegman: abandon the generally used method of index guiding altogether and replace it with gain guiding. He presented the first experimental demonstration of this concept, using a neodymium-doped fiber which is anti-guiding when being unpumped but nevertheless exhibits well-behaved modes due to gain guiding. This was demonstrated with the rather unconventional experimental approach of pumping the fiber with a Xenon flash lamp. While the results are certainly encouraging, with an apparently already rather large mode area, the researchers are not yet able to fully assess the potential of their method [37].

2.5 Design for LMA operation for Waveguides

There are many ways by which LMA operation for waveguides can be done. In all the proposed structure there will be less or no leakage loss for the fundamental mode, whereas there will be significant leakage loss for the higher order modes. One such structure is shown in figure 2.1. Figure 2.1 shows the cross-sectional view of the channel waveguide, which consists of a rectangular core and a geometrically shaped cladding [38]. The core has a high refractive index n_1 , thickness h , and width $2a$, and is formed on a substrate with a lower refractive index n_2 . The region on each side of the core consists of a gradually shaped profile of the same core material. The entire structure is covered by another material with a low index n_3 . As shown in Fig.2.1, the shaped profile starts from a height t at $y = \pm b$ and reaches a height equal to the core thickness h at $y = \pm a$. To facilitate discussion, the shaped profile is described by a power-law expression:

$$x^2(y) = h^2 - (h^2 - t^2) \left\{ \left[\frac{b-y}{b-a} \right]^q \right\}, \text{ for } a \leq y \leq b; \quad (2.1)$$

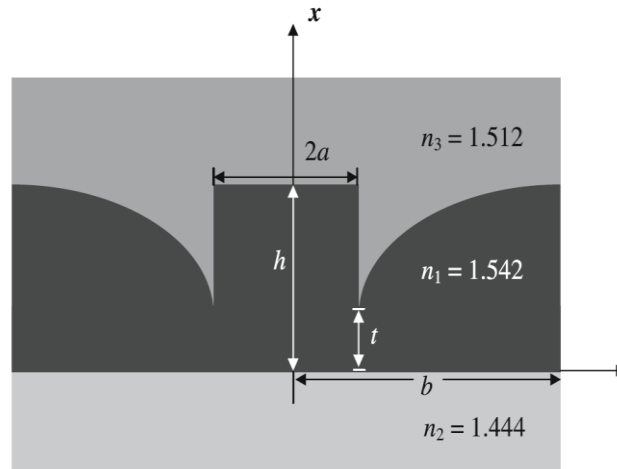


Figure 2.1 Cross-section of a leaky channel waveguide

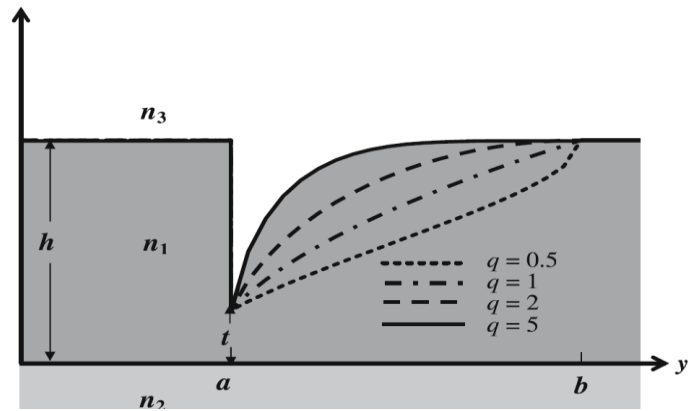


Figure 2.2 Thickness of the cladding varies according to the power-law expression

where $q(> 0)$ is a parameter characterizing the geometric shape of the profile, as shown in Fig 2.2. A similar expression can be written for $-a \geq y \geq -b$. Because the high-index region of the effective cladding eventually reaches the same height as the core, all the modes are leaky. The cladding parameters q , b , and t control the leakage losses of the modes. As will be shown below, such a cladding structure allows single mode operation with a large core and over an extended range of wavelengths. In practice, it is easier to fabricate a step-wise cladding than a gradually shaped cladding. Figure 2.3 shows a stair-case design that consists of four cladding steps with increasing heights.

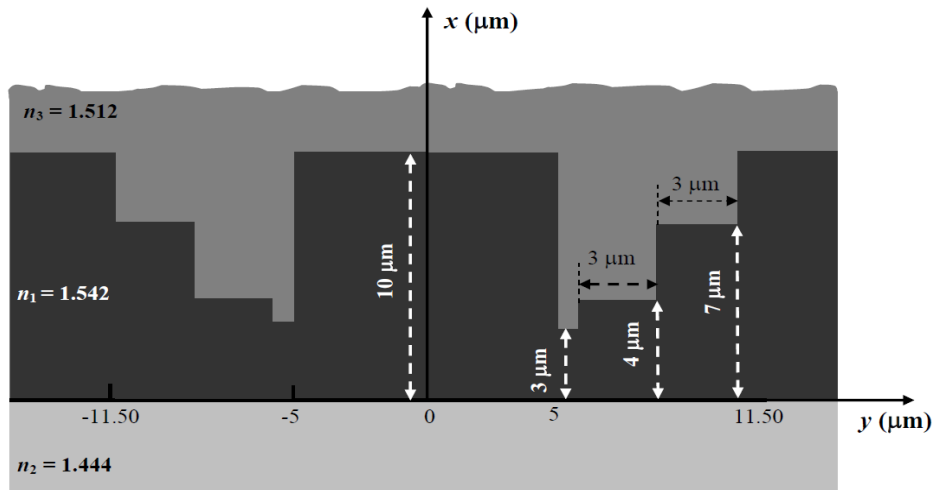


Figure 2.3 Stair-case design of a leaky channel waveguide

Similarly, planar waveguides can also be made to work in single mode operation [39]. One such structure is shown in fig. 2.4. The proposed structure has a uniform substrate, a uniform core and a leaky cladding. The cladding is characterized by a refractive-index profile that increases with the distance from the core. Such a structure supports leaky modes.

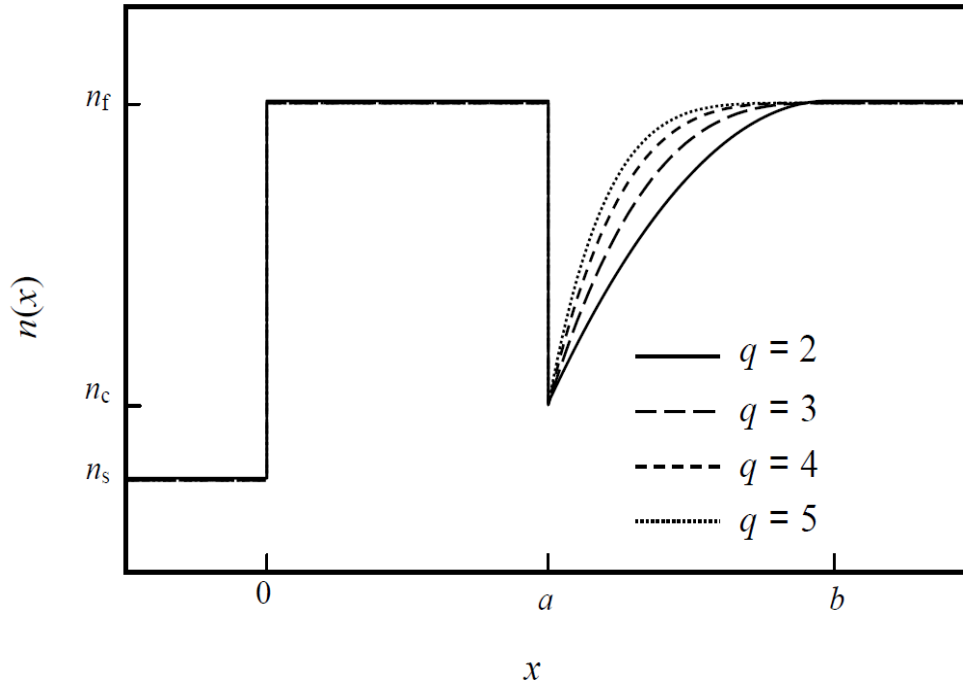


Figure 2.4 *Leaky planar waveguide with a graded-index cladding for different values of profile parameter q .*

In practice, it is easier to fabricate a waveguide with a small number of homogenous layers than one with a continuous graded-index profile. This can also work for a step-wise profile as shown in fig.2.5.

Another proposed structure consists of a uniform substrate, a uniform guiding core and a multi-layer cladding as shown in Fig. 2.5 [40]. The core of width a has the refractive index n_1 , while the cladding of width $(b-a)$ is formed by alternate low and high index regions. The high-index cladding regions have the same refractive-index as that of the core and the refractive-index of the depressed region is subjected to power-law variation given by

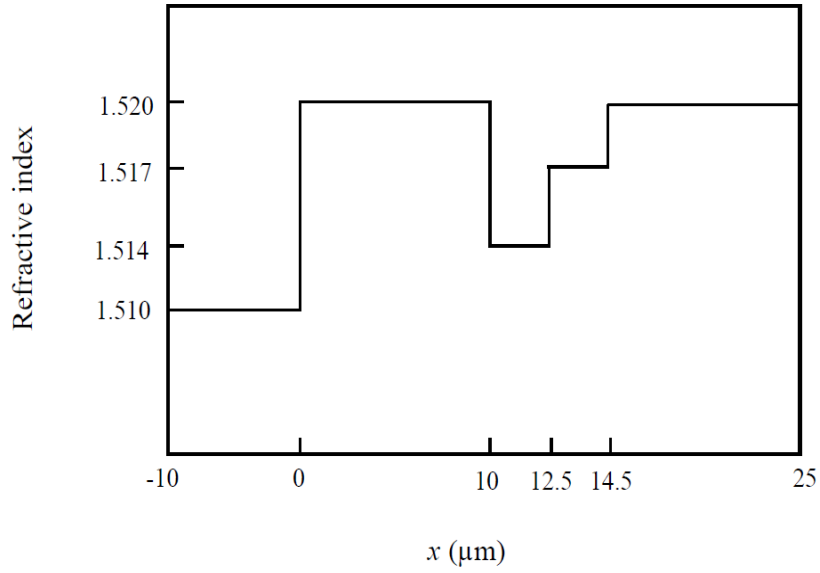


Figure 2.5 *Leaky planar waveguide with only a few cladding layers.*

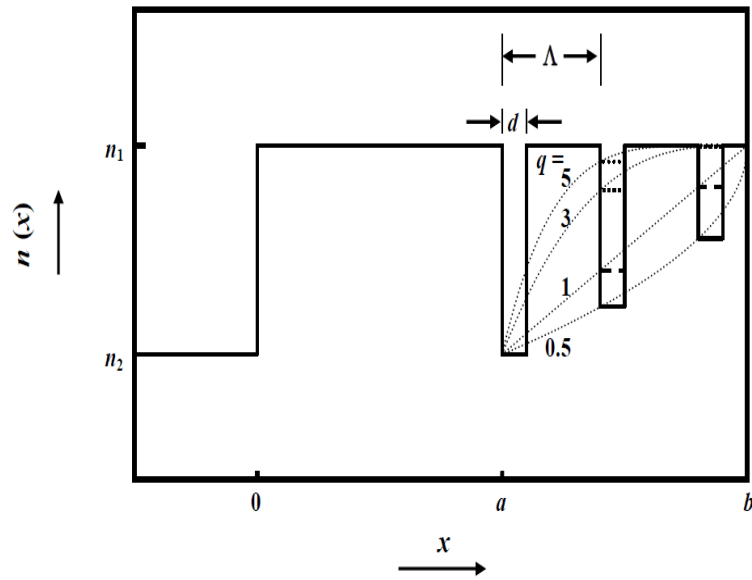


Figure 2.6 *Refractive index profile of multilayer planar waveguide for three different values of profile parameter q.*

$$n^2(x) = n_1^2 \left[1 - 2\Delta \left(\frac{b-x}{b-a} \right)^q \right] \quad ; \text{ for } a < x < b \quad (2.2)$$

Where $q (> 0)$ is called the profile shape parameter. $\Delta = \frac{n_1^2 - n_0^2}{2n_1^2}$ is the relative index difference between guiding core and the first cladding layer, n_2 being the refractive index of the first depressed layer of the cladding. The NA of the waveguide can, thus, be defined as $n_1 \sqrt{2\Delta}$. d represents the width of depressed cladding layer while the periodicity of the low- and high- index cladding layers is defined by Λ .

Chapter 3

Method of analysis

3.1 Introduction

Ongoing developments in the area of optoelectronic design have required accurate, reliable and powerful tools for the analysis of its constitute wave guiding elements as well as for entire circuits. Typical dielectric waveguides which have been developed for optoelectronics are shown in Fig.3.1 and include slab waveguides, buried waveguides, air-clad rib and buried rib waveguides, diffused waveguides and buried diffused waveguides. The analysis of the above mentioned waveguides means finding the propagation constants and field profiles of all the modes that the waveguide supports.

With improvements in computer capabilities there is strong interest and demand for CAD applications that would enhance analysis and play an important part in the design process. Therefore, developing a CAD application package that can provide exact, fast and efficient analysis of the aforementioned components is an area of great interest and research. Unfortunately, with the exception of the simple structure of a slab waveguide, for which exact closed form solutions exist, most practical structures are more complex and exact analytical solutions do not exist. Solution is then sought by solving Maxwell's equations using either numerical or semi-analytical methods. The accent will be put on the semi-analytical methods which form the basis of the present work and on numerical methods that are used to provide results for comparison purposes.

We will be studying both numerical and semi analytical methods in detail in this chapter, while we have taken Effective Index Method (EIM) for analyzing waveguide structures.

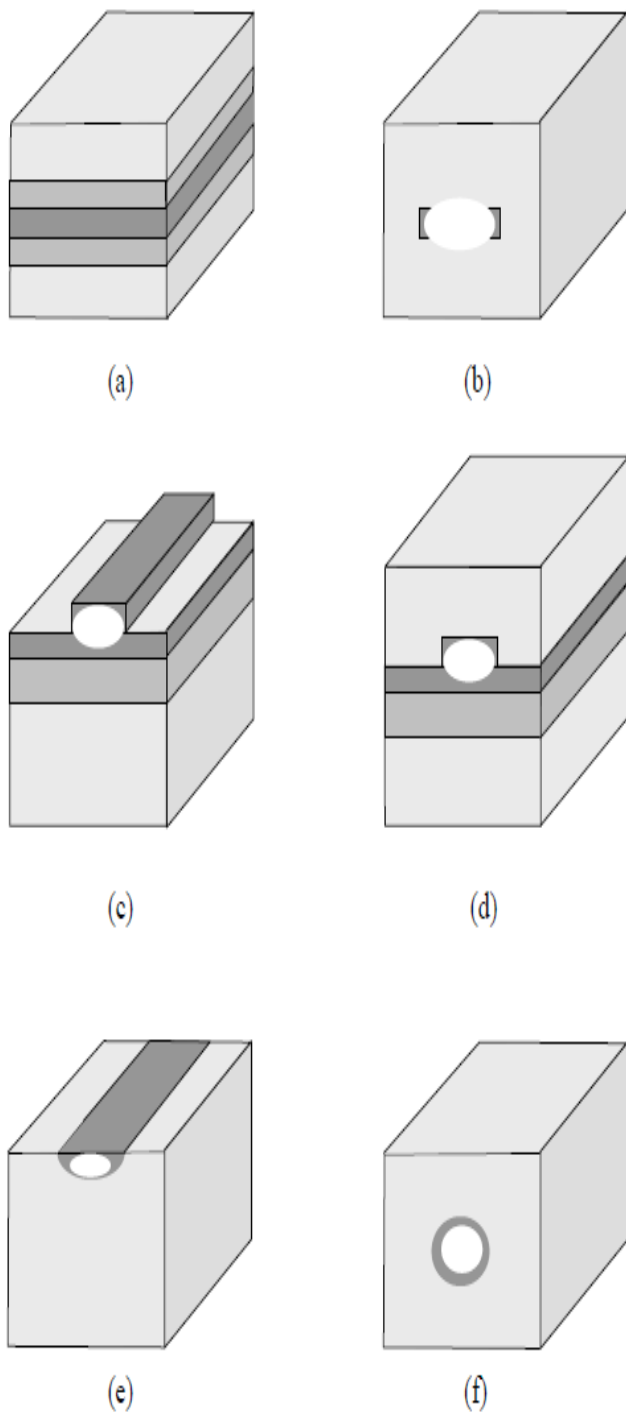


Fig.3.1. Typical dielectric waveguides: (a) slab waveguide, (b) buried waveguide, (c) air-clad rib waveguide, (d) buried rib waveguide, (e) diffused waveguide, (f) buried diffused waveguide

3.2 Numerical methods

Numerical methods solve Maxwell's equations exactly and the results they provide are often regarded as benchmarks. Numerical methods, such as the Finite Difference (FD), Finite Elements (FE) and Finite Difference Beam Propagation (FDBPM) methods are robust, versatile and applicable to a wide variety of structures. Unfortunately, this is often achieved at the expense of long computational times and large memory requirements, both of which can become critical issues especially when structures with large dimensions are considered or when used within an iterative design environment. In this section, a short overview of these numerical methods is given.

3.3 Finite Element method

The Finite Element (FE) method is well established numerical technique for solving boundary value problems. The method is based upon dividing the problem region into non-overlapping polygons, usually triangles, as shown in Fig.3.2. The field over each element is then expressed in terms of low-degree interpolating polynomials weighted by the field values at the nodes of each element. The total field is found as a linear summation of the fields over each element [41,42]. The FE method uses a variational expression which is formulated from Maxwell's equations. By differentiating the variational functional with respect to each nodal value, the eigen value problem is obtained of the form

$$[A][x]-\lambda[B][x]=0 \quad (3.1)$$

where $[A]$ and $[B]$ are sparse matrices, usually symmetric, $[x]$ is the nodal matrix and λ is the natural eigenvalue of the problem. Eq.(3.1) is solved for all eigenvalues using iterative techniques. Solution of the problem can be in terms of its natural frequency or in terms of the propagation constant β , depending on the variational formulation[42]. The former case is less preferred since an initial guess for β is required which can be especially difficult in situations where β has a complex value.

The accuracy of the FE method can be increased by using a finer mesh or by employing higher order polynomials. A finer mesh increases the size of the matrices $[A]$

and [B], and higher order polynomials reduce their sparsity involving increased programming effort.

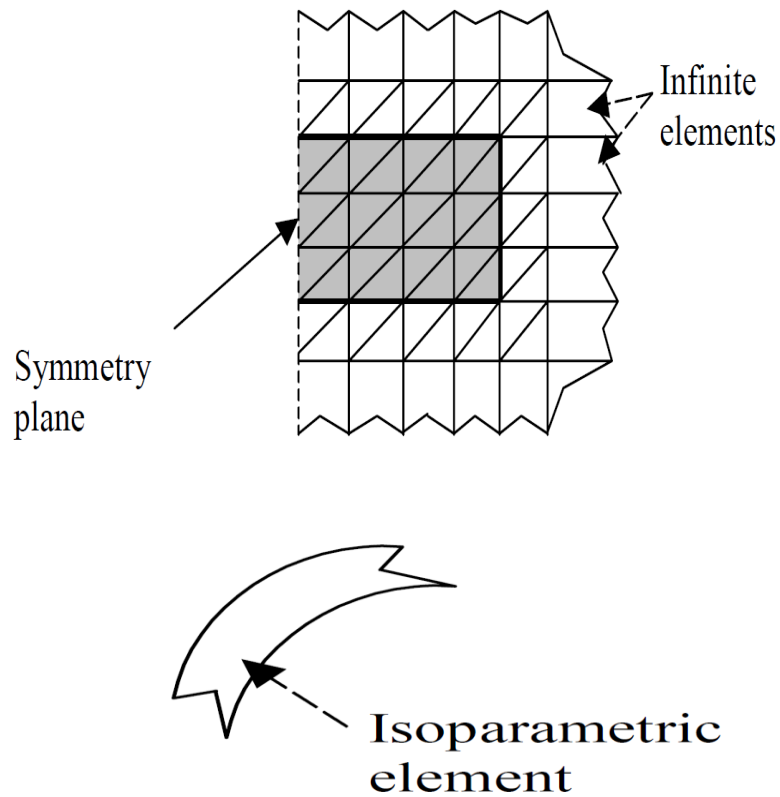


Fig.3.2. Modeling of a buried waveguide using a Finite Element mesh

The appearance of spurious solutions is a serious downside of the method and is caused by not satisfying the divergence condition ($\nabla \cdot \mathbf{H} = 0$). Formulating the variational expression in terms of various field components has been tried to avoid spurious solutions. The number of formulations have been proposed, out of which the full H-field formulation is the most

commonly used in modeling optical waveguides due to a much easier treatment of boundary conditions. However, the occurrence of spurious solution is still present. Until now, only a formulation in terms of the transverse components of the E or H field does not give spurious solutions but it produces dense matrices instead [43-45]. Suppression of spurious solutions can be alternatively achieved by introducing a penalty term into the variational expression with a penalty parameter defined heuristically [46], or by checking the zero divergence condition for each obtained mode and discarding ones that do not satisfy it [47]. These methods are only partially successful since spurious solutions may appear in the whole frequency spectrum and distinguishing them from physical modes can be a very difficult task. A more successful approach is to use edge elements that force spurious solutions exactly at zero frequency [48,49]. In this approach, the interpolating functions are defined as vectors and the continuity of tangential components across elements is satisfied. The continuity of normal field components is not satisfied which gives rise to a non-zero divergence. However, all spurious solutions are forced to zero frequency and hence easily identifiable.

Modeling of the open problem space within the FE method was at first done by truncating the computational window and imposing an artificial electric wall around it, a technique which as with the FD method, gives erroneous results for waveguides operating near cut-off [45]. Much better results were obtained by introducing infinite elements in which the field is forced to decay exponentially (the decay rate being defined heuristically). The infinite elements, (Fig.3.2), do not increase the size of the matrices [50] but on the other hand can treat only nonradiating structures [42, 51]. A better approach is by using an impedance boundary condition where the appropriate radiation condition of the fields at the fictitious boundary (the boundary that separates the interior (guiding) region from the exterior (decaying) region), is assumed and approximately satisfied and from which the condition at the infinity is derived. This approach can also treat the radiation modes by simply allowing complex values of propagation constant. In modeling of complex geometries, the FE method is considered more flexible than the FD method, due to the greater flexibility of triangular elements. The modeling of curved boundaries is additionally eased by use of isoparametric elements, (Fig.3.2), that allow curved edges [52]. However,

for simple geometries, the FD method is reported to be more efficient than the FE method [53].

3.4 Finite Difference Beam Propagation Method

Unlike the above methods, the Beam Propagation method (BPM) describes the evolution of the total field propagating along a guide. The BPM method was first applied to optoelectronics in 1980 [54]. The original BPM represented the total field as a superposition of plane waves that propagate in a homogeneous medium. The propagation was modeled using a paraxial wave equation, which assumes that the wave vector is inclined by a small angle with respect to the axis of propagation [55]. The field that propagates in an inhomogeneous media was calculated by integrating the fields in the spectral domain and applying the phase correction in spatial domain at each propagation step. The Fast Fourier Transform (FFT) was used to relate the spatial and spectral domains, so the method is referred to as FFT-BPM.

Initially, the FFT-BPM was developed for the case of weakly guiding structures, neglecting the vectorial properties of the field. The use of the paraxial approximation limited the method to structures where the beam propagates in directions that make small angle with respect to the axis of propagation. In order to avoid the use of the FFT, the paraxial wave equation was solved through the appropriate variational expression using the FE method [56] and later using the FD method [57] from which the Finite Difference Beam Propagation Method (FD-BPM) evolved. Comparisons between the FFT- and the FD-BPM show that for comparable accuracy the FD-BPM employs larger propagation step size. Also the computational time per propagation step in the FD-BPM is much lower which makes it a more efficient tool for the analysis of complex structures [58].

With the FD implementation, the BPM was soon extended to include vectorial properties for 2D and 3D propagation [59-64]. Recently, FD-BPM schemes based on structures related co-ordinate schemes that naturally follow the geometry of a structure have been described and shown to be particularly useful when the angle between the waveguide and propagation direction increases [65]. From the aspect of modeling the open

boundary condition at the edge of the problem work space, absorbing boundary conditions (ABC) were first applied [66]. These have subsequently been replaced by efficient transparent boundary conditions (TBC) [67]. In the ABC approach unwanted reflections are absorbed by a lossy material that is placed at the edges of computation window. The major disadvantage of the ABC is that the lossy material is problem dependent and fields at the boundary must have zero value so that a large computational time and computer memory are frequently required. In the TBC approach the outgoing wave is let pass at a particular incident angle. This method is less problem dependent, more robust and does not require large memory resources. Still, the window size should be sufficiently large as not to cause power attenuation of the part of the field that propagates in the core region [68]. Also, the effectiveness of the TBC approach is limited for structures with wide angle propagating waves.

Recently, a new boundary condition, the perfectly matched layer (PML) boundary condition, has been proposed and reported to be the most effective[69,70]. The PML approach is based on introducing a fictitious layer of certain electric conductivity that is able to absorb and exponentially attenuate the outgoing wave at any angle or frequency. The Finite Difference Beam Propagation Method (FD-BPM) is one of the most popular methods for analysis of field propagation in inhomogeneous optical guides like tapers, Y-junctions, bends and gratings.

3.5 Analytical Methods

This section will present an alternative approach to the numerical methods discussed in the previous section. The analytical methods are widely used in the modeling of optoelectronic waveguides such as buried waveguides, rib waveguides, tapers and directional couplers. Unlike numerical methods, semi-analytical methods make certain approximations to the structure under consideration and then solve the resulting, simplified problem analytically. This group of methods has always been very popular with the optoelectronic circuit designer, especially before the advent of modern computers. Since they are very efficient, often provide accuracy comparable with that of numerical methods and are also easily

implemented, they are still highly valuable for the design of a particular device or even entire circuits. Unfortunately, each semi-analytical method is usually limited to a certain type or class of problem. The number and scope of semi-analytical methods is rapidly increasing, with both the development of new methods and the improvement of existing ones. Methods such as the mode-matching method, transverse resonance methods, perturbation methods, the method of lines, the Effective Index method, and the Spectral Index method all belong to the class of semi-analytical methods[45,71]. To give a proper account of every method is beyond the scope of this thesis and therefore this section will only focus on those methods which are closely related to this work.

3.6 Effective Index Method

Effective Index (EI) method [72] is one of the most popular methods for the analysis of optical waveguides. In this method, the effective index of the structure is obtained by successively solving two transcendental slab equations. If the example of a rib waveguide is considered, Fig.3.3(a), then the method in the first step solves transcendental equations for three vertical slabs, Fig.3.3(b). The effective indices (n_{eff1}) so obtained become the refractive indices for a horizontal slab waveguide, as shown in Fig.3.3(c). Solving the transcendental equation for the horizontal slab gives a good approximation to the effective index of the original rib waveguide structure. The advantage of the EI method is that it can be applied to a wide variety of structures. The weakness of the method is that it does not give good results when the structure operates near cut-off or when the outer slab of a rib guide is not a guiding slab [45]. Moreover, the field profiles obtained from the method is of limited use. The simplicity and speed of the method have encouraged many engineers to search for different approaches that will improve the accuracy of the EI method. Consequently, many different variants of the EI have been developed such as the EI method based on linear combinations of solutions [73, 74], the EI method with perturbation correction [75], or the variational EI method developed specifically for rib waveguide analysis.

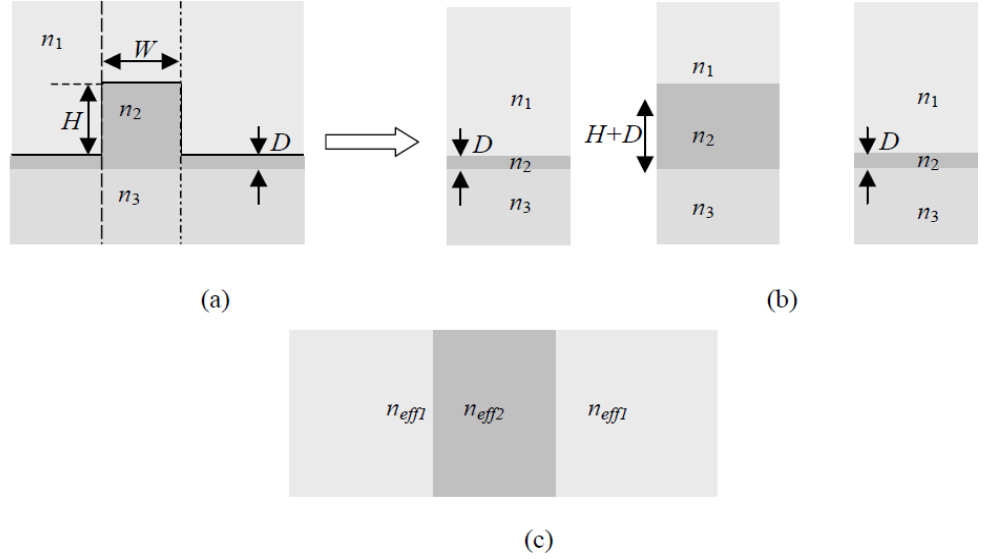


Fig.3.3 The Effective Index method for the rib waveguide (a) the original rib waveguide, (b) solving the vertical slab problem to define n_{eff1} and n_{eff2} (step 1), (c) solving the equivalent horizontal slab problem for n_{eff} of the whole structure (step 2).

We will be using EIM in conjunction with TMM (Transfer Matrix Method). Leakage loss of higher order modes and the guiding property of the fundamental mode have been analyzed by calculating the propagation constant, leakage loss and the modal field profile of the modes by using TMM. TMM is a powerful tool to analyze the propagation characteristics of fiber and waveguides having arbitrary shape. Being a scalar method, it is fast and easy to implement. This method is particularly useful for analyzing a multilayer structure such as the one proposed in this paper. By applying suitable boundary conditions at the interface of two consecutive layers, the field coefficients in the layers can be related by a 2×2 matrix, usually referred to as a transfer matrix. The field coefficients of the first and the last layer of the profile can be connected by simply multiplying all the intermediate matrices of each interface. A suitable boundary condition in the first and last layer would lead to a complex eigenvalue equation. Any suitable root searching algorithm can be used to solve the complex roots of the equation. The real part of the propagation constant gives

information about the effective index of a mode while the leakage loss can be estimated from the imaginary part.

Chapter 4

Design and Analysis of Leaky Channel Waveguide

For large mode area design, we have proposed a leaky design so that only fundamental mode experiences no loss while other mode experiences loss. Hence by this design fundamental mode propagates through the core. The structure is shown in the figure 4.1.

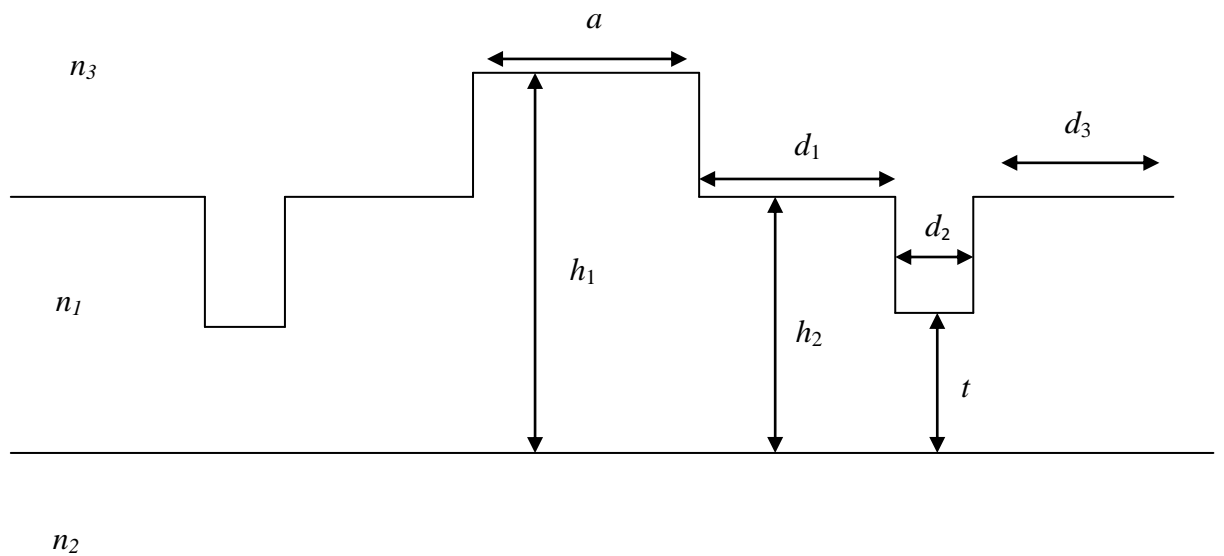


Figure 4.1: *Proposed Leaky structure*

The proposed structure channel waveguide is characterized by uniform rectangular core; namely central and side core; and a leaky cladding. The central core has a high refractive index n_1 , a thickness h_1 , and a width a , while side core which is placed on the each side of central core has same refractive index n_1 , thickness h_2 and width d_1 . Both the cores are formed on a substrate with a lower index n_2 . The region on each side of the core consists of a stair-case profile of the same core material. The stair stops at a

height equal to the side core thickness t . The entire structure is covered by another material with a low index n_3 .

Proposed channel waveguide is designed in such a way that it supports that it supports several modes out of which only fundamental mode is perfectly guiding rest others are leaky in nature. A 20dB leakage loss to the first higher order mode can strip off all the higher order to ensure the effective single-mode operation is calculated by solving the structure by using Effective Index method in conjunction with Transfer Matrix Method. All the parameters play a crucial role in designing the waveguide for large mode area effective single-mode operation.

In EIM, since the proposed structure is two dimensional structures, hence analysis can be done through EIM method in conjunction with TMM method. The analysis can be done in either of two ways i.e. y - method or x -method. We will solve it using x - method. Under this method, first the given structure is solved in y –axis and then it is solved in x -axis, hence making two- dimensional structure into one – dimensional structure and then we will apply TMM method.

We have now optimized the values of different parameters in such a way that only fundamental mode is able to propagate, while other mode experiences loss. In this we have observed the variation of losses with change in: wavelength, a , d_1 , d_2 , t .

We have carried out numerical simulation for the following parameters unless stated otherwise, which are typical for silica on silicon waveguides $n_1= 1.542$, $n_2= 1.444$, $n_3= 1.512$;

$$a = 5\mu\text{m}, d_1 = 5\mu\text{m}, d_2 = 1\mu\text{m}, d_3 = 10\mu\text{m}, h_1 = 10\mu\text{m}, h_2 = 7\mu\text{m}, t = 3\mu\text{m}.$$

Contour plot and field plot of E_{11}^x and E_{21}^x is shown below. In the same way field plot of E_{11}^y and E_{21}^y is also shown. With the help of contour and field plot, losses of desired modes can be found easily among undesired and number of modes.

To make the complete study of the proposed design, we have studied the effect of all design parameter for single mode operation.

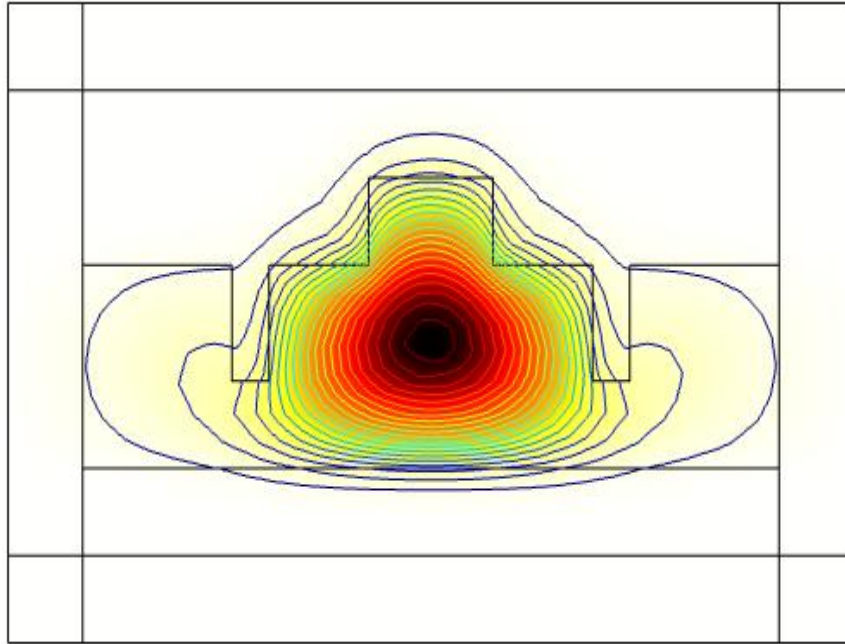


Fig.4.2: *Contour plot of E_{11}^x*

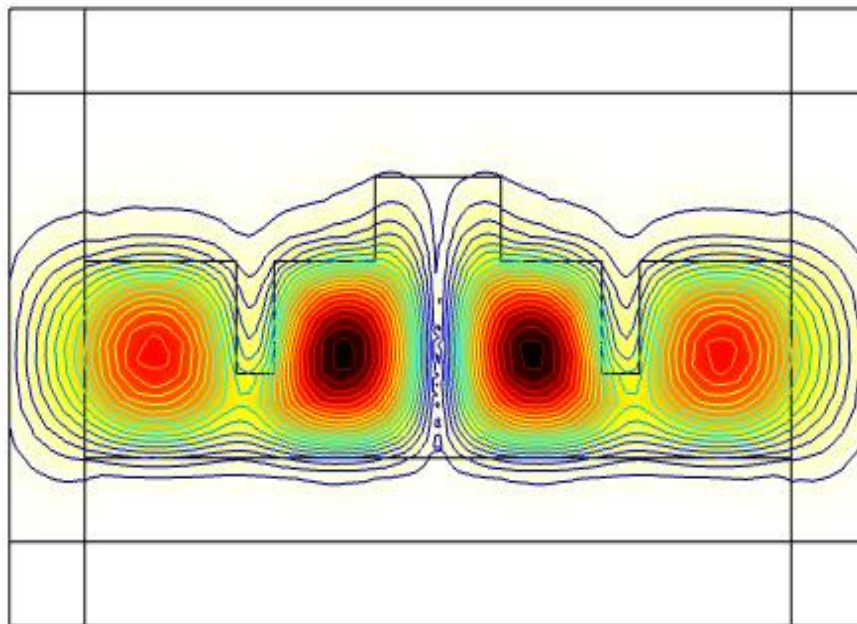


Fig.4.3: *Contour plot of E_{21}^x*

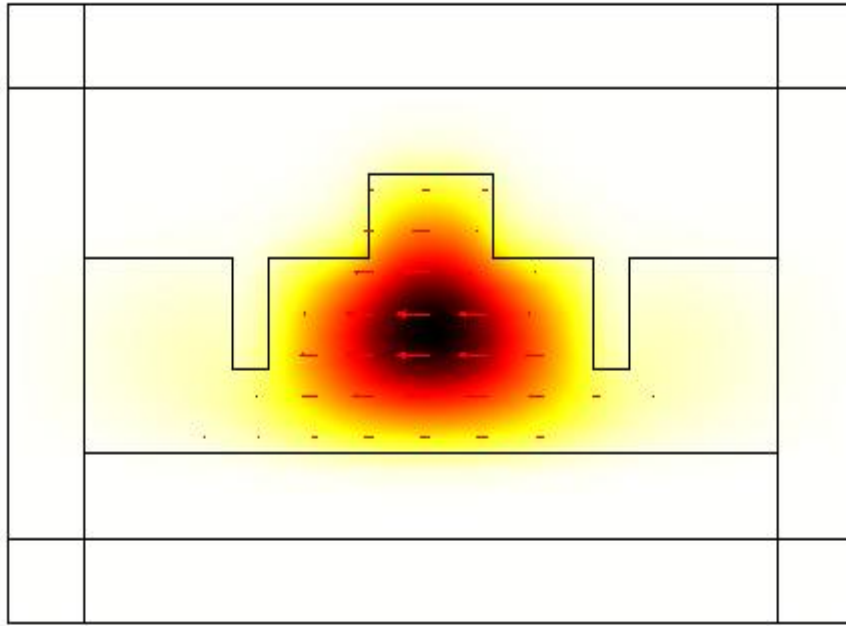


Fig.4.4: *Field plot of E_{11}^x*

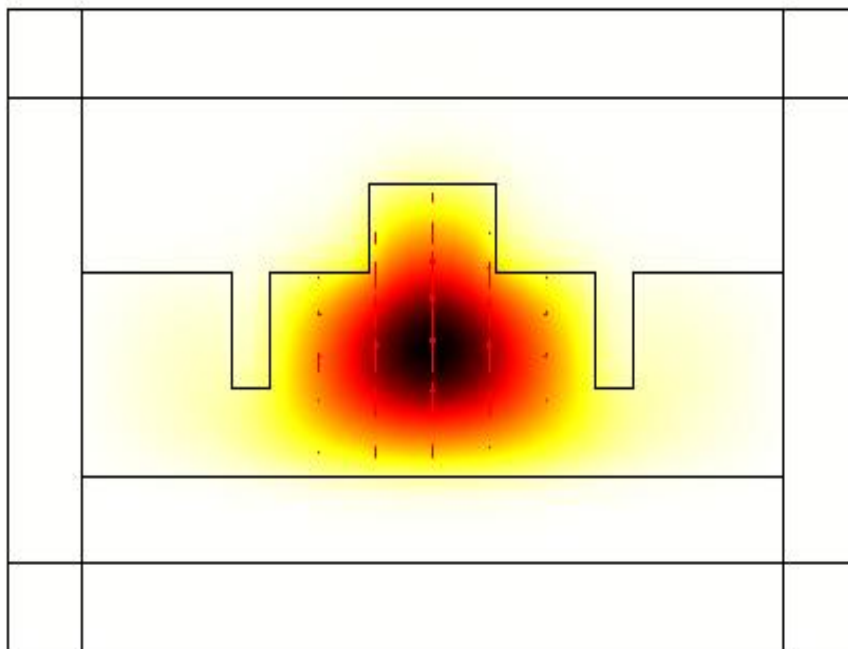


Fig.4.5: *Field plot of E_{11}^y*

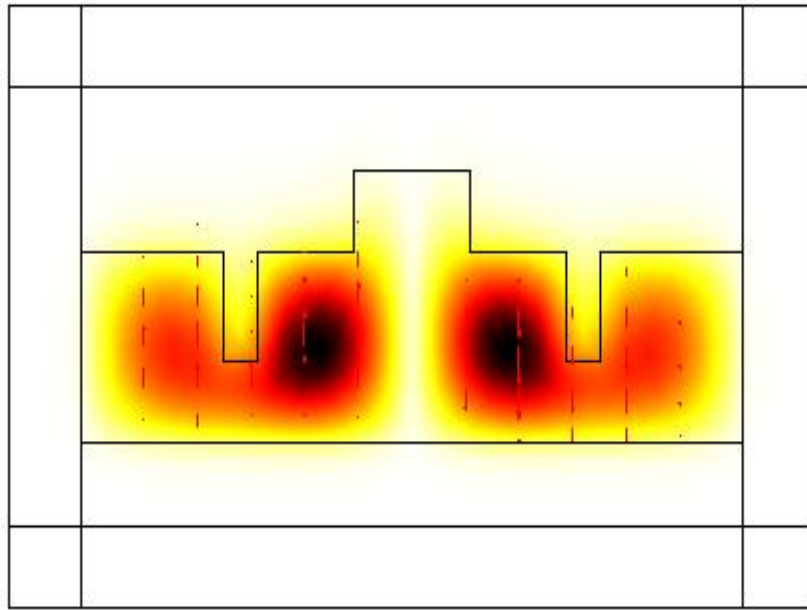


Fig.4.6: *Field plot of E_{21}^y*

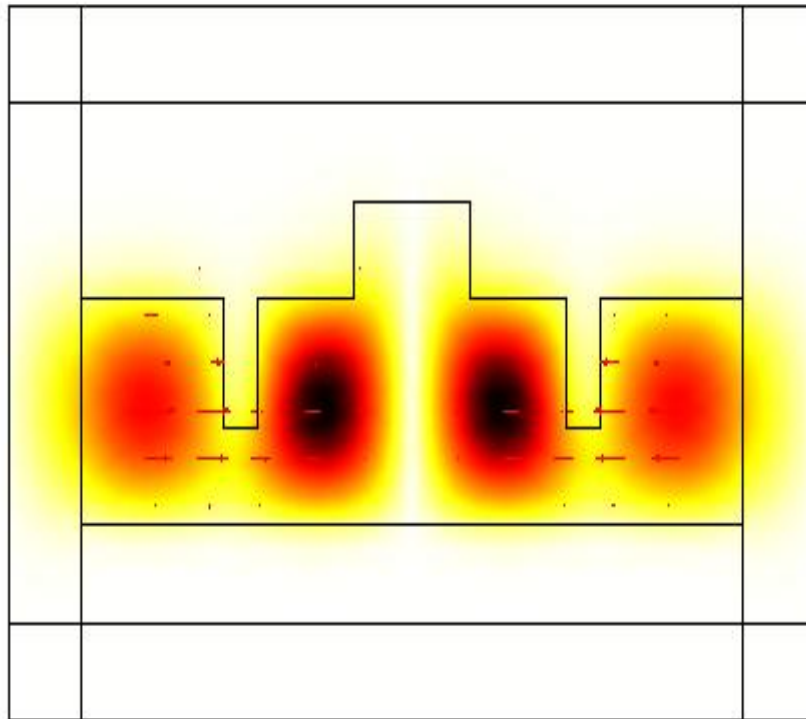


Fig.4.7: *Field plot of E_{21}^x*

We have optimized the different parameters of the design.

Firstly optimizing the value of d_1 in which value of d_1 is changed from 1 micron to 5 micron, keeping all the parameter constant at $\lambda = 1.55 \mu\text{m}$. Variation of leakage loss of higher order modes with change in value of d_1 is shown in fig.4.8.

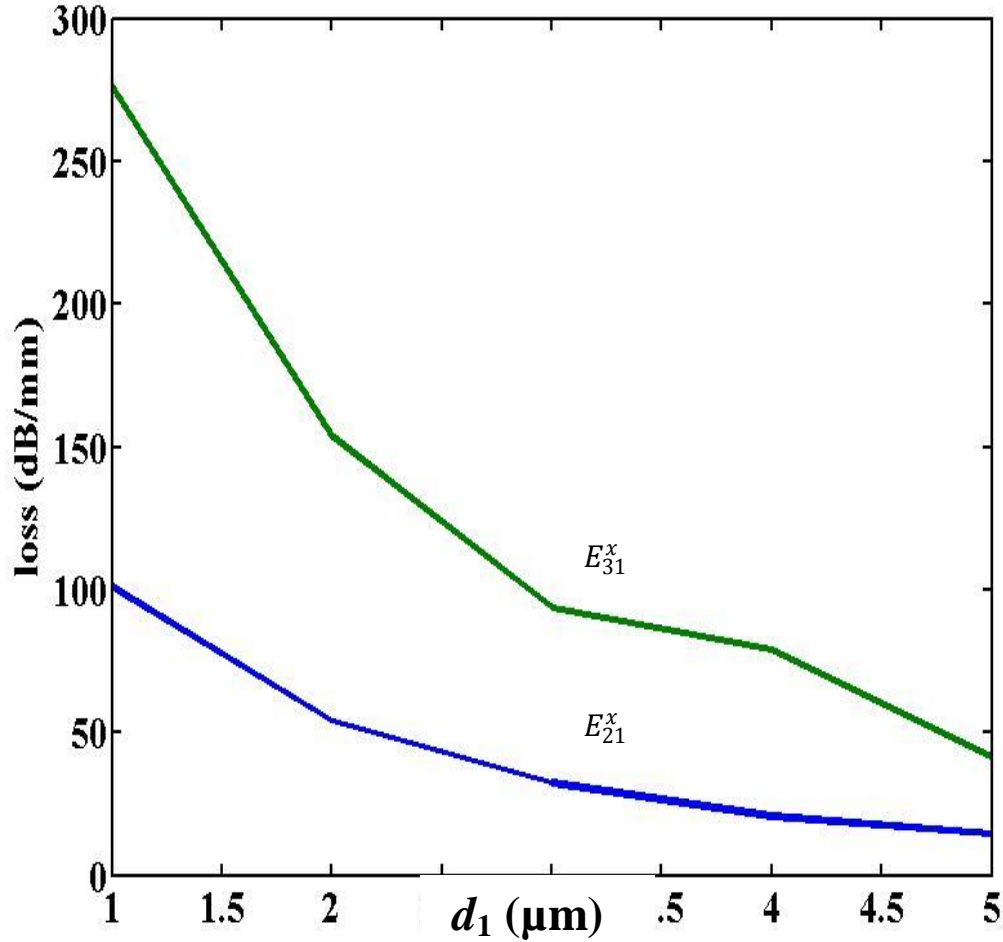


Fig.4.8: Variation of leakage loss of E_{21}^x and E_{31}^x with change in value of d_1

As seen from the graph that as the distance d_1 increases, leakage loss decreases. In addition to this, leakage loss increases as the mode order increases. It is because as the distance of high refractive index region from low refractive index region increases, hence less loss will be experienced due to abrupt change in refractive index region. In another words, when less distance is there between high index region and low index region, it makes higher order modes to leak out hence, making leakage loss increased for higher order modes. It can be observed from graph that at $d_1=5$ micron loss

experienced by E_{21}^x is approximately 20dB/mm, hence 1mm of distance is required to leaked out higher order modes.

Variation of mode area of E_{21}^x is shown in figure 4.9.

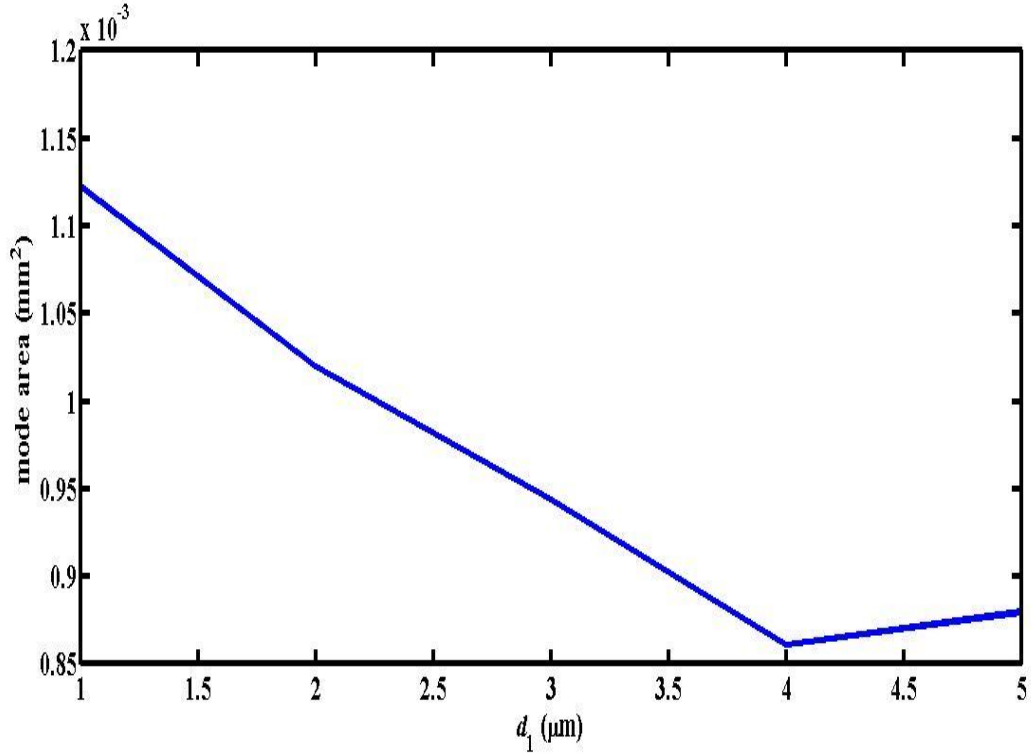


Fig.4.9: Variation of mode area of E_{21}^x with change in value of d_1

From the graph it can be observed with increase in value of d_1 , mode area of E_{21}^x decreases, since larger mode area shows that mode will be spread in leaky region, and hence loss increases. It was seen that mode area at $d_1= 5$ micron is $905 \mu\text{m}^2$.

Now the value of d_2 is optimized, hence for this the value of d_2 is varied from 0.5 micron to 2.5 micron at $\lambda= 1.55 \mu\text{m}$. It can be seen from the graph as d_2 increases, leakage loss decreases. It is because for small values of d_2 , there will be abrupt change in refractive index profile, hence experiencing more leakage loss. Whereas when large value of d_2 is observed, there will be smooth transition from high index region to low index region. Therefore less loss is experienced. It is to be further noted that loss experienced by the higher order modes are large compared to that of lower order modes. It was seen that leakage loss of E_{11}^x was experiencing no loss, whereas losses of higher

order modes were significant, which could be verified by the graph of leakage loss of E_{21}^x with change in value of d_2 as shown in fig.4.10.

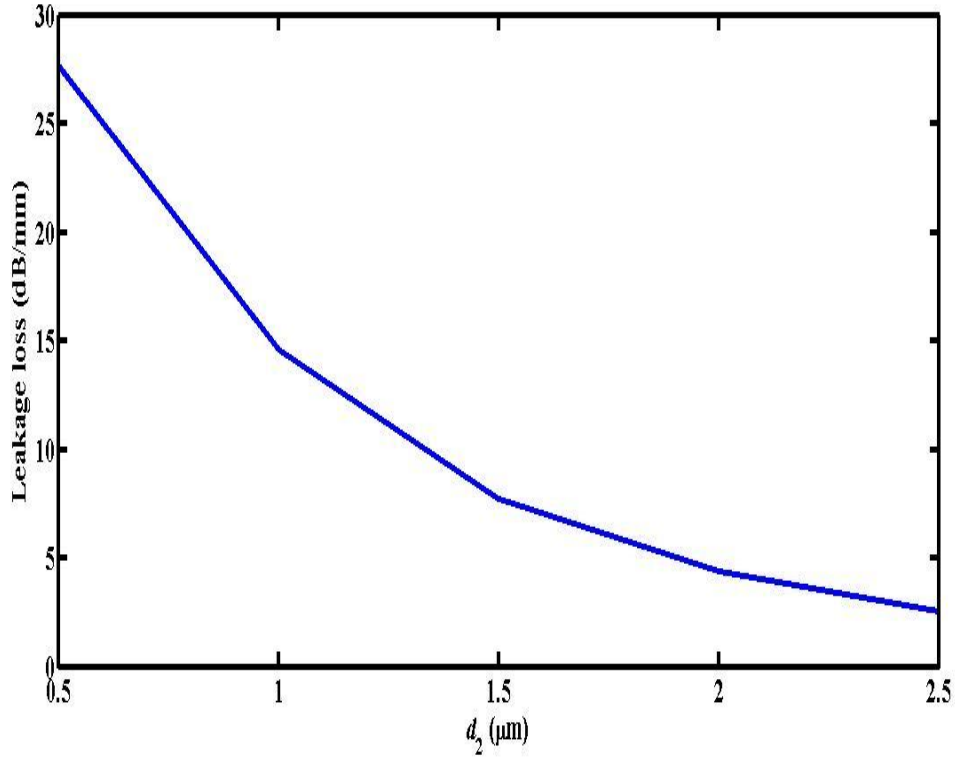


Fig.4.10: Variation of leakage loss of E_{21}^x with change in value of d_2

It can be seen from the figure that at $d_2 = 1.5 \mu\text{m}$, loss experienced by higher order modes was approximately 8dB/mm, which in turn shows that higher order modes will require 3mm of length of waveguide, to completely leaked out higher order modes. It means that a waveguide of length 3mm can efficiently show single mode operation.

Variation of mode area of E_{21}^x with change in d_2 is shown in figure 4.11. It can be seen that as d_2 increases, mode area of E_{21}^x decreases and at $d_2 = 2$ micron mode area is equal to $874 \mu\text{m}^2$. On further increasing d_2 value, mode area gets constant hence making it optimized for the value of d_2 .

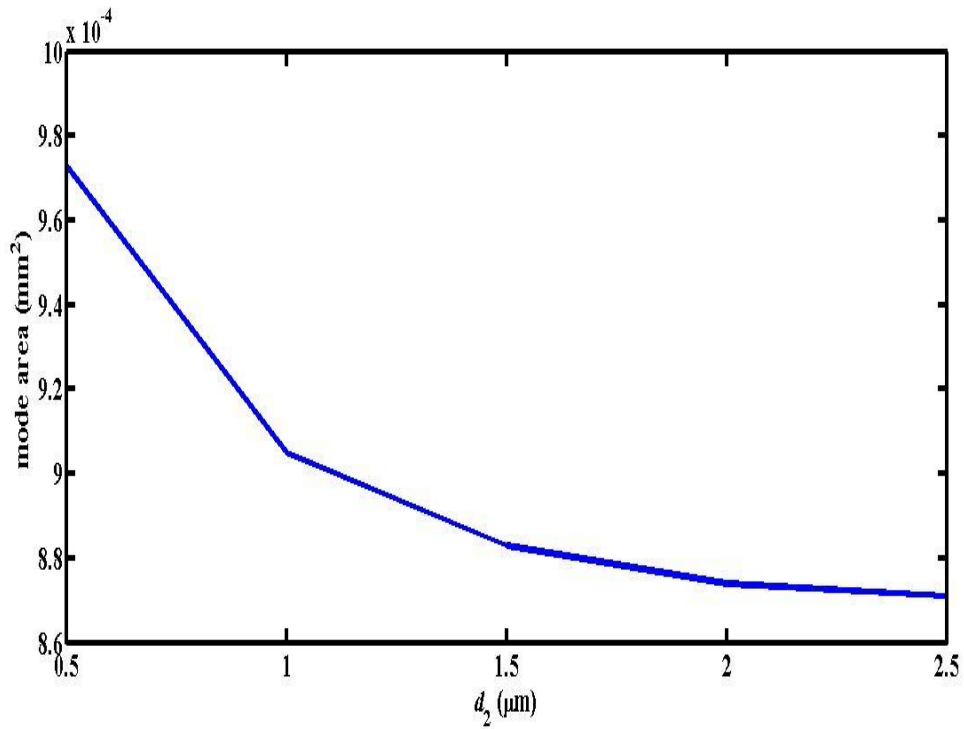


Fig.4.11: Variation of mode area of E_{21}^x with change in value of d_2

After optimizing the value of d_1 , d_2 we will be optimizing values of a and t . Here value of t is optimized. This is done by varying the value of t from 1 to 5 micron, while keeping all the parameters constant.

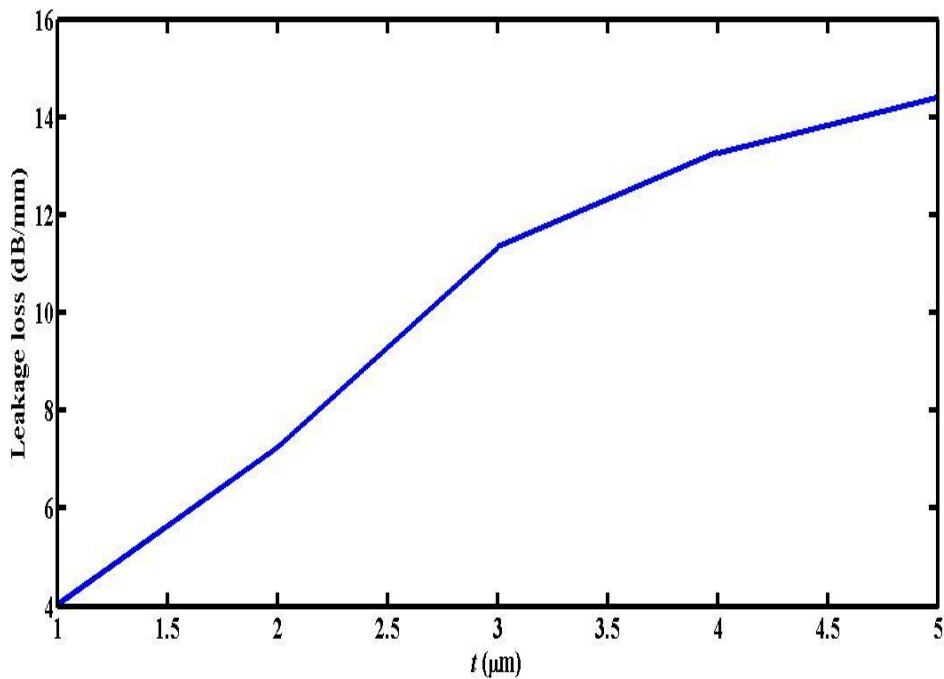


Fig.4.12: Variation of leakage loss of E_{21}^x with change in 't'

As seen from the graph that as the t increases, so is the loss associated with it. Loss associated with higher order modes was large as compared to lower order modes. An increase in the value of t effectively decreases the core-cladding index contrast and thus increases the losses of the modes. At $t = 5$ micron, loss associated with E_{21}^x is 15 dB/mm, hence approximately 1.4 mm of distance is required to completely leak out E_{21}^x , which makes waveguide to efficiently work as single mode operation. It is also to be noted that at $t = 5$ micron, loss also becomes constant, optimizing the value for t .

Variation of mode area of E_{21}^x with change in t is shown in figure 4.13. It increases as value of t increases. At $t = 5$ micron mode area is equal to $942 \mu\text{m}^2$.

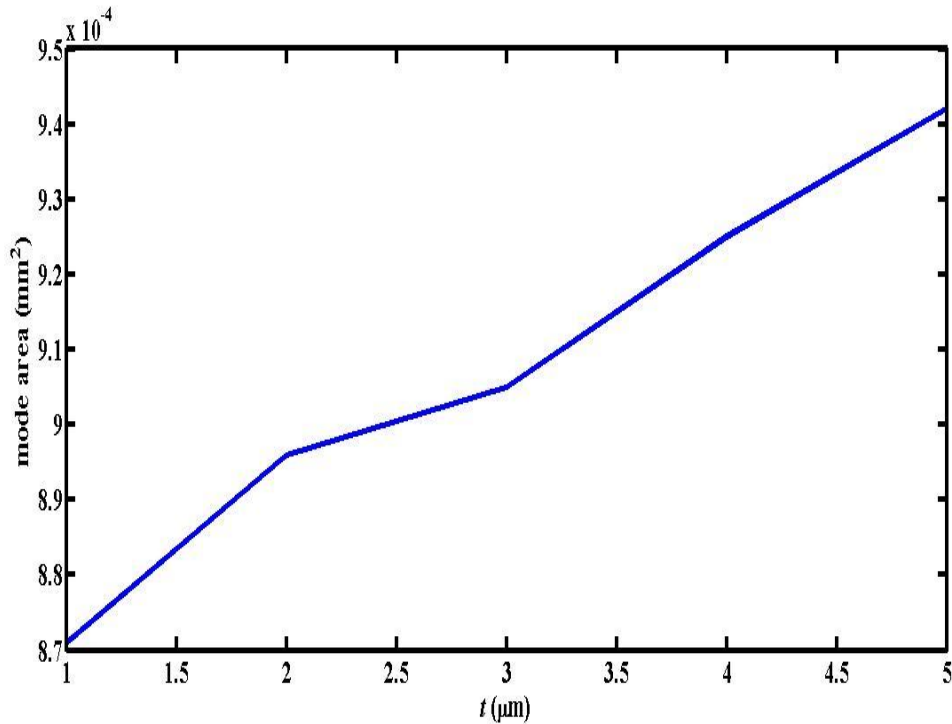


Fig.4.13 Variation of mode area of E_{21}^x with change in t

Now 'a' is optimized by varying the length from 5 micron to 9 micron, keeping all the parameters constant. As observed from the graph as 'a' increases, leakage loss decreases. Leakage loss of higher order mode is high as compared to E_{21}^x . An increase in the core width leads to a tighter light confinement in the core and hence a lower leakage loss. Hence a must be around 7 micron to leak out higher modes, which is having loss of 8 dB/mm. Therefore it will require length of 2.5 mm to completely leak out higher order modes.

Variation of mode area with change in a is shown in fig.4.15. It can be seen from the graph that as a increases, mode area also increases. At $a = 9$ micron, mode field area is equal to $1085\mu\text{m}^2$.

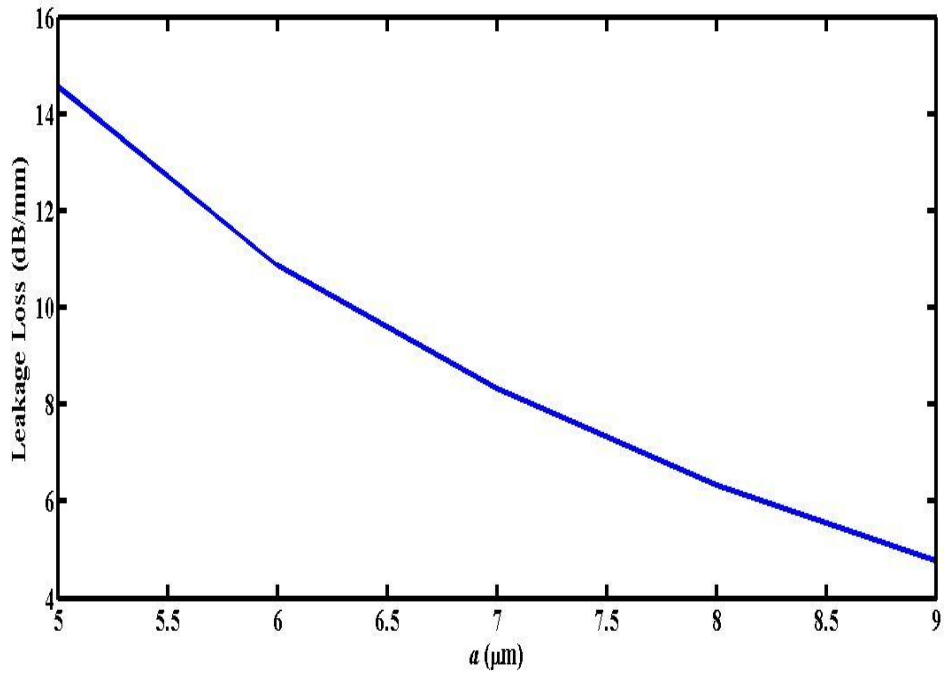


Fig.4.14: Variation of leakage loss of E_{21}^x with change in 'a'

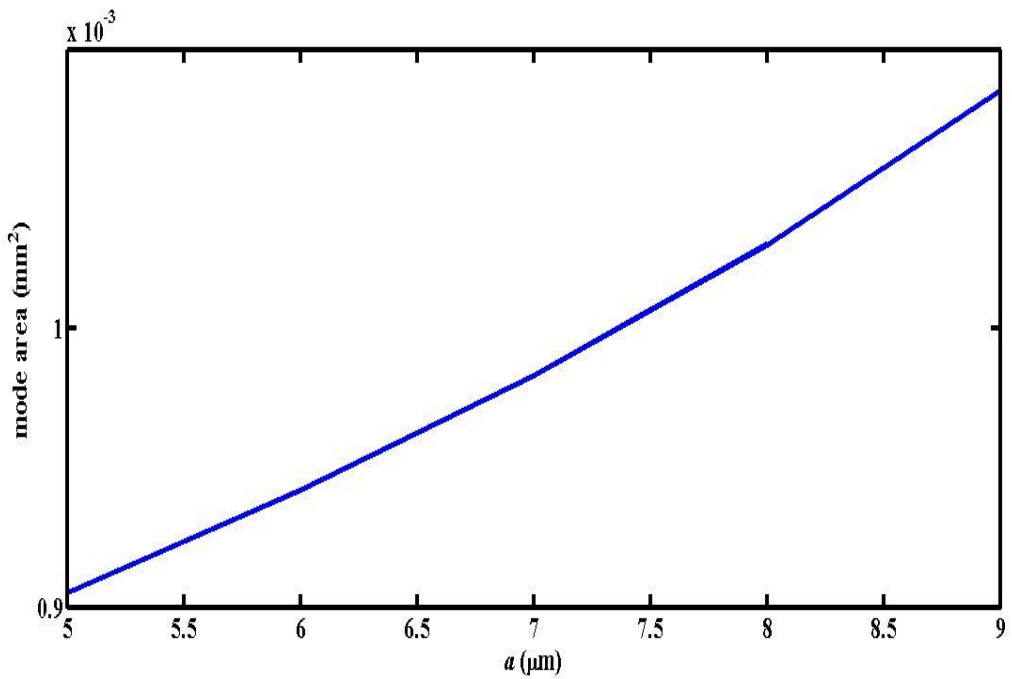


Fig. 4.15: Variation of mode area of E_{21}^x with change in a

After optimizing the parameters of the structure, spectral analysis is being observed.

Fig.4.16 shows the effective-index profiles $n_{eff}(y)$ calculated for two different wavelengths $\lambda = 633 \text{ nm}$ and $\lambda = 1550 \text{ nm}$.

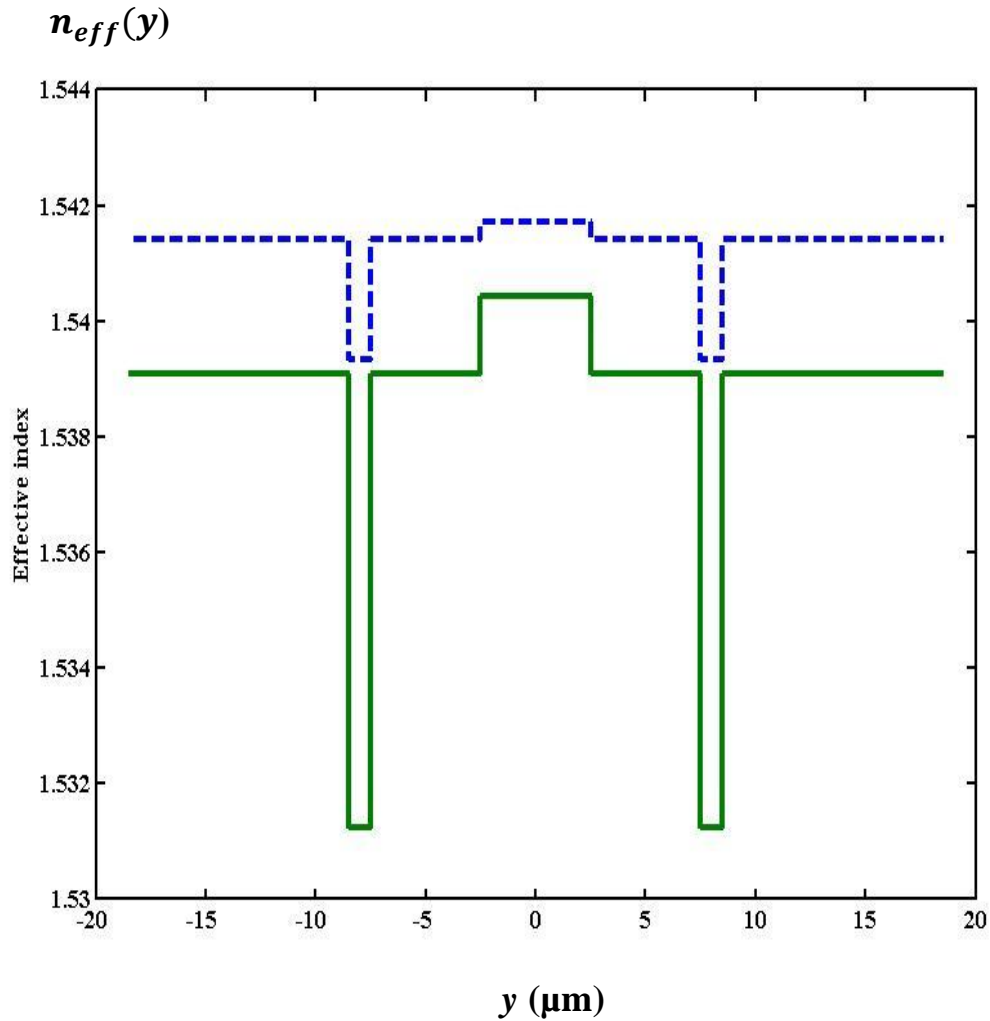


Fig.4.16: One-dimensional effective refractive-index profiles obtained by the effective-index method for the wavelengths 633 nm (dashed) and 1550 nm (solid)

As shown in Fig.4.16, the index of the cladding increases monotonically in the x -direction and eventually reaches the same value of the core index. In such a structure, the effective index of each mode is lower than the cladding index at a certain distance from the core and thus becomes leaky. If the leakage losses of all the high-order modes are significantly larger than that of the fundamental mode, the structure operates effectively as a single-mode waveguide.

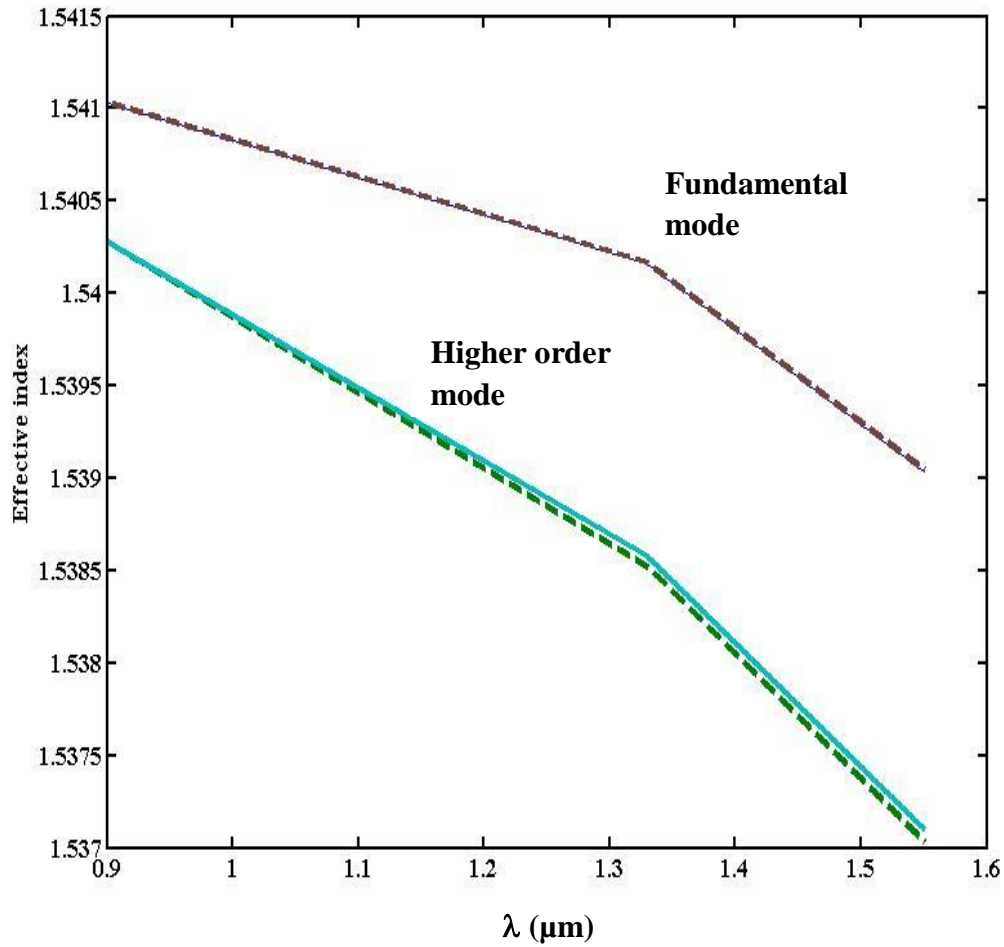


Fig.4.17: Variation of effective index of E_{11}^x and E_{21}^x (solid), E_{11}^y and E_{21}^y (dashed) with change in value of wavelength

As seen by the graph as the wavelength increases effective index decreases. It is because as wavelength increases normalised parameter decreases, which in turn show that wave, will be less confined in core and will spread in leaky region, hence effective index decreases. It is further to be noted that effective index of the fundamental mode i.e. E_{11}^x is high as compared to that of higher order mode E_{21}^x . In the same way graph of effective index of E_{11}^y and E_{21}^y with change in wavelength is also plotted in fig.4.17. It was observed that loss of E_{11}^y and E_{21}^y was less as compared to that of E_{11}^x and E_{21}^x . Hence by analyzing graph of for both x and y polarization, it can be said that both show approximately same characteristics while changing the value of parameters.

Chapter 5

Conclusion and Scope for Future Work

We propose a new class of channel waveguides that can potentially offer single-mode operation with a large core area. The waveguide is characterized by a uniform rectangular core and a geometrically shaped cladding to provide leakage for all the modes. When all the modes, except for the fundamental mode, are stripped off sufficiently in the waveguide, effective single-mode operation is ensured. Single mode operation is made possible with the help of certain design parameters due to which higher order modes are leaked out. Due to large core area it can support large power and is also less fragile. This is a great advantage.

In thesis we came upon following conclusion:

Firstly, as the distance ' d_1 ' increases, the loss associated with it decreases. In addition to this, leakage loss increases as the mode order increases. Secondly, as ' d_2 ' increases, leakage loss decreases. Similarly, as ' t ' increases, so is the loss associated with it. Loss associated with higher order modes was large as compared to lower order modes. And finally, as ' a ' increases, leakage loss decreases, since an increase in the core width leads to a tighter light confinement in the core and hence a lower leakage loss. For the wavelength, as the wavelength increases, loss associated with also increases.

Our numerical example with typical design parameters shows that such a waveguide can provide single-mode operation with a core area as large as $100 \mu\text{m}^2$ over an extended range of wavelengths, which can effectively suppress nonlinear optical effects and increase the power-handling capacity of the waveguide. Waveguide would be effectively single mode after travelling a distance of $\approx 2.5 \text{ mm}$. This class of waveguide is expected to find applications in high-power waveguide lasers and amplifiers.

It was seen that for extended single mode operation a/h_1 ratio must be between 0.5 to 1 [76], which is also verified as our ratio came out to be 0.7.

References

1. G. P. Agarwal, "Fiber-optic communication system", John Wiley & sons.
2. A. Ghatak and K. Thyagrajan, "Introduction to fiber optics".
3. J. M Senior, "Optical fiber Communication".
4. Katsunari Okamoto, "Fundamental of Optical Waveguide".
5. J. M. Eggleston, J. J. Kane, K. Kuhn, J. Unternahrer and R. L. Byer , IEEE J. Quantum Electron 20, 289-301 (1984).
6. H. L. Offerhaus, N. G. Broderick, D. J. Richardson, R. Sammut, J. Caplen, L. Dong, Opt. Lett. 23, 1683 (1998)
7. G. P. Lees, D. Taverner, D. J. Richardson, L. Dong, T. P. Newson, Electron. Lett. 33, 393 (1997)
8. J. C. Knight, T. A. Birks, R. F. Cregan, P. S. J. Russell, J.P. De Sandro, Electron. Lett. 34, 1347 (1998)
9. V. Rastogi, K.S. Chiang, Opt. Lett. 26, 491 (2001)
10. V. Rastogi, K.S. Chiang, J. Opt. Soc. Am. B 21, 258 (2004)
11. A. Mollo, I. Naeh, Y. Lavi, A. Katzir, Appl. Phys. Lett. 88, 251 101 (2006)
12. M.-C. Oh, S.-H. Cho, Y.-O. Noh, H.-J. Lee, J.-J. Joo, M.-H. Lee, IEEE Photon. Technol. Lett. 17, 1890 (2005)
13. J. M. Heaton, M. M. Bourke, S. B. Jones, B. H. Smith, K. P. Hilton, G. W. Smith, J. C. H. Birbeck, G. Berry, S. V. Dewar, D. R. Wight, J. Lightwave Technol. 17, 267 (1999)
14. V. Rastogi, K.S. Chiang, Electron. Lett. 39, 1110 (2003)
15. A. Kumar, V. Rastogi, K.S. Chiang, Appl. Phys. B 85, 11 (2006)
16. M. E. Fermann, "Single-mode excitation of multimode fibers with ultrashort pulses", Opt. Lett. 23 (1), 52 (1998)
17. H. L. Offerhaus, N. G. Broderick, D. J. Richardson, R. Sammut, J. Caplen, and L. Dong, "High-energy single-transverse-mode Q-switched fiber laser based on a multimode large-mode-area erbium-doped fiber", Opt. Lett. 23 (21), 1683 (1998)

18. J. P. Koplow, D. A. V. Kliner, and L. Goldberg, "Single-mode operation of a coiled multimode fiber amplifier", *Opt. Lett.* 25 (7), 442 (2000)
19. S. Wielandy, "Implications of higher-order mode content in large mode area fibers with good beam quality", *Opt. Express* 15 (23), 15402 (2007)
20. C. Liu, G. Chang, N. Litchinitser, A. Galvanauskas, D. Guertin, N. Jacobson, and K. Tankala, "Effectively single-mode chirally-coupled core fiber", in *Advanced Solid-State Photonics*, OSA Technical Digest Series (CD), paper ME2 (2007)
21. N. Litchinitser, A. Galvanauskas, D. Guertin, N. Jacobson, "Effectively single-mode large core passive and active fibers with chirally coupled-core structures", paper CMB1 at CLEO/QELS 2008, May 4–9, San Jose, CA
22. W. S. Wong, X. Peng, J. M. McLaughlin, L. Dong, "Breaking the limit of maximum effective area for robust single-mode propagation in optical fibers", *Opt. Lett.* 30 (21), 2855 (2005)
23. H. A. McKay, L. Fu, J. Li, H. G. Winful, "Bend-resistant fundamental mode operation in ytterbium-doped leakage channel fibers with effective areas up to $3160 \mu\text{m}^2$ ", *Opt. Express* 14 (24), 11512 (2006)
24. L. Dong, T. Wu, H. A. McKay, L. Fu, J. Li, H. G. Winful, "All-glass large-core leakage channel fibers", *IEEE Sel. Top. Quantum Electron.* 15 (1), 47 (2009)
25. F. Jansen, F. Stutzki, H. J. Otto, T. Eidam, A. Liem, C. Jauregui, "Thermally induced waveguide changes in active fibers", *Opt. Express* 20 (4), 3997 (2012)
26. G. Canat, S. Jetschke, S. Unger, L. Lombard, P. Bourdon, J. Kirchhof, V. Jolivet, A. Dolfi, and O. Vasseur, "Multifilament-core fibers for high energy pulse amplification at $1.5 \mu\text{m}$ with excellent beam quality", *Opt. Lett.* 33 (22), 2701 (2008)
27. S. Ramachandran, J. Fini, M. Mermelstein, J. W. Nicholson, "Light propagation with ultra large modal areas in optical fibers", *Opt. Lett.* 31 (12), 1797 (2006)
28. S. Ramachandran, J. Fini, M. Mermelstein, J. W. Nicholson, S. Ghalmi, "Ultra-large effective-area, higher-order mode fibers: a new strategy for high-power lasers", *Lasers & Photon. Rev.* 2 (6), 429 (2008)
29. A. E. Siegman, "Propagating modes in gain-guided optical fibers", *J. Opt. Soc. Am. A* 20 (8), 1617 (2003)

30. Y. Chen, V. Sudesh, T. McComb, M. Richardson, M. Bass, and J. Ballato, "Lasing in a gain-guided index antiguided fiber", *J. Opt. Soc. Am. B* 24 (8), 1683 (2007)
31. V. Sudesh, T. McComb, Y. Chen, "Diode-pumped 200 μm diameter core, gain-guided, index-antiguided single mode fiber laser", *Appl. Phys. B* 90, 369 (2008)
32. W. Hageman, C. Ying, W. Xiangru, G. Lanlan, K. G. Ug, R. Martin, B. Michael, "Scalable side-pumped, gain-guided index-antiguided fiber laser", *J. Opt. Soc. Am. B* 27 (12), 2451 (2010)
33. Conferences Photonics West in San Jose talk 6453-48
34. Conferences Photonics West in San Jose talk 6453-15
35. Advanced Solid-State Photonics (ASSP) in Vancouver talk ME2
36. Conferences Photonics West in San Jose talk 6453-42 and Advanced Solid-State Photonics (ASSP) in Vancouver talk ME3
37. Dr. R. Paschotta, "Continuing Struggle for Larger Fiber Mode Areas"
38. A. Kumar, V. Rastogi and K. S. Chiang, "Large-core single-mode channel waveguide based on geometrically shaped leaky cladding," *Applied Physics B*, vol. 90, pp. 507-512, 2008.
39. A. Kumar, V. Rastogi and K. S. Chiang, "Leaky optical waveguide for high power applications," *Applied Physics B*, vol. 85, pp. 11-16, 2006
40. A. Kumar, V. Rastogi, "Multilayer cladding leaky planar waveguide for high power applications," *Applied Physics B*, vol. 92, pp. 577-583, 2008.
41. M. N. O. Sadiku, "Numerical techniques in electromagnetics", CRC Press Inc., 1992
42. F. Fernandez, Y. Lu, "Microwave and optical waveguide analysis by the Finite Element method", Research Studies Press Ltd., 1996.
43. F. Fernandez, Y. Lu, "Variational Finite Element analysis of directional waveguides with no spurious solutions", *Electronics Lett.*, 26, pp.2125-2126, 1990.
44. B. M. Dillon, J. P. Webb, "A comparison of formulations for the vector finite element analysis of waveguides", *IEEE Trans. Microwave Theory Tech.*, 42, pp.308-316, 1994.

45. K. S. Chiang, "Review of numerical and approximate methods for the analysis of general optical dielectric waveguides", *Optical and Quantum Electronics*, 26, pp.S113-S134, 1994.
46. B. M. A. Rahman, J. B. Davies, "Penalty function improvement of waveguide solution by finite elements", *IEEE Trans. Microwave Theory Tech.*, 32, pp.922-928, 1984.
47. B. M. A. Rahman, J. B. Davies, "Finite element analysis of optical and microwave waveguide problems", *IEEE Trans. Microwave Theory Tech.*, 32, pp.20-28, 1984
48. M. Koshiha, K. Inoue, "Simple and efficient finite-element analysis of microwave and optical waveguides", *IEEE Trans. Microwave Theory Tech.*, 40, pp.371-377, 1992.
49. J. F. Lee, D. K. Sun, Z. J. Cendes, "Full-wave analysis of dielectric waveguides using tangential vector finite elements", *IEEE Trans. Microwave Theory Tech.*, 39, pp.1262-1271, 1991.
50. C. Yeh, K. Ha, S. B. Dong, W. P. Brown, "Single-mode optical waveguides", *Appl. Optics*, 18, pp.1490, 1979.
51. H. E. Hernandez-Figueroa, F. A. Fernandez, J. B. Davies, "Finite element approach for the modal analysis of open boundary waveguides", *Electronics Lett.*, 30, pp.2031-2032, 1994.
52. M. Egushi, M. Koshiha, "Accurate Finite-Element analysis of dual mode highly elliptical core fibres", *J. Lightwave Technol.*, 12, pp.607-613, 1994.
53. S. S. Patrick, K. J. Webb, "A variational vector Finite Difference analysis for dielectric waveguides", *IEEE Trans. MTT*, 40, pp.692-698, 1992.
54. M. D. Fiet, J. A. Fleck, Jr., "Computation of mode eigenfunctions in graded index optical fibres by the beam propagation method" *Appl. Optics*, 19, pp.2240-2246, 1980.
55. H. A. Haus, "Waves and fields in optoelectronics", Englewood Cliffs, NJ: Prentice Hall, pp.99-103, 1984.
56. T. B. Koch, J. B. Davies, D. Wickramasinghe, "Finite element finite difference propagation algorithm for integrated optical device", *Electronics Lett.*, 25, pp.514-516, 1989.

57. S. T. Hendow, S. A. Shakir, "Recursive numerical solution for nonlinear wave propagation in fibres and cylindrically symmetric systems", *Appl. Optics*, 25, pp.1759-1764, 1986.
58. Y. Chung, N. Dagli, "An assessment of finite difference beam propagation method", *IEEE J. of Quantum Electronics*, 26, pp1335-1339, 1990.
59. W. P. Huang, C. L. Xu, S. T. Chu, S. K. Chaudhuri, "A vector beam propagation method for guided wave optics", *IEEE Photon. Tech. Lett.*, 3, pp.910-913, 1991.
60. W. P. Huang, C. L. Xu, S. T. Chu, S. K. Chaudhuri, "A finite difference vector beam propagation method: analysis and assessment", *IEEE/OSA J. Lightwave Technol.* 10, pp.295-305, 1992.
61. P. L. Liu, B. J. Li, "Study of form birefringence in waveguide devices using the semivectorial beam propagation method", *IEEE Photon. Tech. Lett.*, 3, pp.913-915, 1991.
62. P. L. Liu, B. J. Li, "Semivectorial beam propagation method for analyzing polarized modes of rib waveguides", *IEEE J. Quantum Electron.*, 28, pp.778- 782, 1992.
63. W. P. Huang, C. L. Xu, S. K. Chaudhuri, "A vector beam propagation method based on H-fields", *IEEE Photon. Tech. Lett.* 3, pp.1117-1120, 1991.
64. W. P. Huang, C. L. Xu, S. K. Chaudhuri, "A finite difference vector beam propagation method for three dimensional waveguide structures", *IEEE Photon. Tech. Lett.*, 4, pp.148-151, 1992.
65. T. M. Benson, P. Sewell, S. Sujecki, P. C. Kendall, "Structure related beam propagation", *Optical and Quantum Electronics*, 31, pp.689-703, 1999.
66. P. E. Lagasse, R. Baets, "Application of propagating beam methods to electromagnetic and acoustic wave propagation problems: a review", *Radio Sci.*, 22, pp.1225-1233, 1987.
67. R. G. Hadley, "Transparent boundary condition for beam propagation methods", *Opt. Lett.*, 16, pp.624-626, 1991.
68. W. P. Huang, C. L. Xu, L. Yokoyama, "The perfectly matched layer (PML) boundary condition for the Beam Propagation Method", *IEEE Photonics Techn. Lett.*, 8, pp.649-651, 1996.

69. F. Akleman, L. Sevgi, "A novel implementation of Berenger's PML for FDTD applications", IEEE Microwave and Guided Wave Lett., 8, pp.324- 326, 1998.
70. C. Vassalo, "1993-1995 Optical mode solvers", Optical and Quantum Electronics, 29, pp.95-114, 1997.
71. R. M. Knox, and P. P. Toullos, "Integrated circuits for the millimeter through optical frequency range", Proc. M.R.I. Symp. Submillimeter waves, Fox J., Ed. Brooklyn, N.Y.: Polytechnic Press, pp.497-516, 1970.
72. K. S. Chiang, "Dual Effective Index method for the analysis of rectangular dielectric waveguides", Appl. Opt. 25, pp.2169-2174, 1986.
73. J. J. G. M. Van Der Tol, N. H. G. Baken, "Correction to Effective Index method for rectangular dielectric waveguides", Electron. Lett., 24, pp.207-208, 1988.
74. K. S. Chiang, "Analysis of rectangular dielectric waveguides: Effective-Index method with built-in perturbation correction", Electron. Lett., 28, pp.388-390, 1992.
75. T. M. Benson, R. J. Bozeat, P. C. Kendall, "Rigorous EI method for semiconductor optical rib waveguides", IEE Proc. J., 139, pp.67-70, 1992.
76. R. A. Soref, J. Schmidtchen, and K. Petermann, "Large Single-Mode Rib Waveguides in GeSi-Si and Si-on-SO₂", IEEE journal of Quantum Electronics Vol. 27. No. 8. August 1991.